Title
Protection of cell therapeutics from antibody-mediated killing by CD64 overexpression.

Journal
Nature biotechnology, 41(5)

ISSN
1087-0156

Authors
Gravina, Alessia
Tediashvili, Grigol
Rajalingam, Raja
et al.

Publication Date
2023-05-01

DOI
10.1038/s41587-022-01540-7

Peer reviewed

nature biotechnology

Article

https://doi.org/10.1038/s41587-022-01540-7

Protection of cell therapeutics from antibody-mediated killing by CD64 overexpression

Received: 28 August 2021

Accepted: 3 October 2022

Published online: 02 January 2023

Check for updates

Alessia Gravina[1], Grigol Tediashvili[1], Raja Rajalingam[2], Zoe Quandt[3], Chad Deisenroth[4], Sonja Schrepfer[1] & Tobias Deuse[1]

Allogeneic cell therapeutics for cancer therapy or regenerative medicine are susceptible to antibody-mediated killing, which diminishes their efficacy. Here we report a strategy to protect cells from antibody-mediated killing that relies on engineered overexpression of the IgG receptor CD64. We show that human and mouse iPSC-derived endothelial cells (iECs) overexpressing CD64 escape antibody-dependent cellular cytotoxicity (ADCC) and complement-dependent cytotoxicity from IgG antibodies in vitro and in ADCC-enabled mice. When CD64 expression was combined with hypoimmune genetic modifications known to protect against cellular immunity, $B2M^{-/-}CIITA^{-/-}$ CD47/CD64-transgenic iECs were resistant to both IgG antibody-mediated and cellular immune killing in vitro and in humanized mice. Mechanistic studies demonstrated that CD64 or its intracellularly truncated analog CD64t effectively capture monomeric IgG and occupy their F_c, and the IgG bind and occupy their target antigens. In three applications of the approach, human CD64t-engineered thyroid epithelial cells, pancreatic beta cells and CAR T cells withstood clinically relevant levels of graft-directed antibodies and fully evaded antibody-mediated killing.

The concept of antibody-mediated rejection (AMR) after solid organ transplantation became a focus in transplant research in the 1990s, decades after the concept of cellular rejection had been widely accepted. A hallmark of AMR is the presence of graft-specific antibodies[1] in combination with graft damage. The emergence of such antibodies occurs despite the use of guideline-driven systemic immunosuppression. Outside of transplantation, some autoimmune diseases are characterized by autoantibodies that mediate the destruction of the target cells and persist even after the affected cell population has vanished. The emergence of antibodies against allogeneic cell therapeutics has been observed in clinical trials[2–4]. Cancer therapy with chimeric antigen receptor (CAR) T cells induces antibodies, especially if tumor cell types other than B cells or plasma cells are targeted[5]. It is, therefore, likely that most allogeneic cellular grafts for long-term regenerative or oncology indications in immunocompetent patients will eventually experience some form of antibody-mediated killing. We, therefore, sought to develop a gene engineering approach that provides antibody protection for cell therapeutics.

For both antibody-mediated cellular cytotoxicity (ADCC) and complement-dependent cytotoxicity (CDC), antibodies of the IgG class mediate target cell killing by binding an epitope via their antigen-binding fragments (F_{ab}) and activating effector cells or

[1]Transplant and Stem Cell Immunobiology (TSI) Laboratory, Department of Surgery, University of California, San Francisco, San Francisco, CA, USA. [2]Immunogenetics and Transplantation Laboratory, Department of Surgery, University of California, San Francisco, San Francisco, CA, USA. [3]Department of Medicine, Division of Diabetes, Endocrinology and Metabolism, University of California, San Francisco, San Francisco, CA, USA. [4]United States Environmental Protection Agency, Center for Computational Toxicology & Exposure, Durham, NC, USA. e-mail: tobias.deuse@ucsf.edu

complement via their free fragment crystallizable domain (F_c). We hypothesized that forced overexpression of the high-affinity receptor for IgG F_c (CD64) on graft cells would capture monomeric IgG F_c and make F_c inaccessible for effector cells or complement. IgG against epitopes expressed on these cells could bind and occupy those. We found that the protection that CD64 overexpression reliably established was effective against ADCC and CDC, was agnostic to the specific type of cell and was applicable to three clinically relevant cell therapeutics.

Results

Cd64-expressing mouse iECs are protected from antibody-mediated killing

Mouse C57BL/6 (B6) induced pluripotent stem cells (iPSCs) were differentiated into B6 iECs, and the cells were transduced with lentiviral particles to express the mouse Cd64 transgene. B6 iECs^{Cd64} were able to bind free mouse IgG2a F_c in a concentration-dependent manner (Supplementary Fig. 1a,b). In mice, IgG2a and IgG2b are the main antibody isotypes mediating ADCC and CDC. For these F_c binding assays, antibodies are used that are specific for an epitope that is not expressed on the cells to avoid any specific F_{ab} binding. The flow cytometry signal then only measures antibodies captured via F_c. For in vitro killing assays, B6 iECs and B6 iECs^{Cd64} were grown on electrode plates for real-time impedance cytotoxicity assays with B6 natural killer (NK) cells as effector cells (ADCC) or B6 serum (CDC). In this highly sensitive assay, target cell death leads to a disruption of the cell covering of electrodes with a decrease of impedance and drop of the plotted cell index curve.

We used a mouse IgG2a antibody against the B6 major histocompatibility complex (MHC) haplotype H-2^b and found that it effectively mediates ADCC and CDC against B6 iECs. Engineered B6 iECs^{Cd64} were fully protected against ADCC and CDC (Supplementary Fig. 1c,d).

In a next step, we modified B6 *B2m*$^{-/-}$*Ciita*$^{-/-}$Cd47$^+$ hypoimmune (HIP; Supplementary Fig. 2a) iECs[6] to additionally express human CD64 (B6 HIP iECs^{CD64}). HIP cells are protected from allogeneic innate and adaptive immune cell killing[6,7] but are potentially susceptible to antibody-mediated killing. To design a very stringent model, target cells were additionally transduced to express human CD52, the target for the highly cytotoxic anti-CD52 antibody alemtuzumab (Supplementary Fig. 2b). B6 HIP iECs^{CD64} showed human IgG1 F_c capture ability in a concentration-dependent manner (Supplementary Fig. 2c). In ADCC and CDC assays with anti-CD52, B6 HIP iECs^{CD52} were killed by mouse NK cells and complement even at low antibody concentrations. This confirmed the high cytotoxic capacity of alemtuzumab and its functional compatibility with mouse NK cells and complement. B6 HIP iECs^{CD52,CD64} were fully resistant against ADCC and CDC across the anti-CD52 concentration spectrum (Supplementary Fig. 2d,e).

Next, grafts of 1 million firefly luciferase-positive (Luc$^+$) B6 HIP iECs^{CD52} and B6 HIP iECs^{CD52,CD64} were transplanted subcutaneously into Rag-1-deficient mice. This strain lacks mature B and T cells but has functional NK cells[8] and serves well as an ADCC in vivo model. Two alemtuzumab doses at 1 mg each were injected into the peritoneum on post-transplant days 0 and 3. Graft survival was followed by bioluminescence imaging (BLI) (Supplementary Fig. 2f). We saw the B6 HIP iECs^{CD52} grafts vanish within approximately 1 week, whereas B6 HIP iECs^{CD52,CD64} grafts survived and were protected from ADCC (Supplementary Fig. 2g,h). The ability of CD64 to capture F_c was thus shown to add antibody protection to mouse HIP cells in vivo and in vitro.

CD64-expressing human iECs are protected from antibody-mediated killing

Human iECs of the HLA-A*02:01 genotype were transduced to overexpress human CD64 using lentiviral particles, and cells with high CD64 expression (iECs^{CD64}) were enriched using cell sorting (Fig. 1a). Their ability to capture human IgG1 F_c in a concentration-dependent manner was shown (Fig. 1b). In vitro killing assays were performed using a recombinant human anti-HLA-A2 IgG1 antibody[9] with human NK cells as effector cells (ADCC) or human serum (CDC). Whereas iECs underwent increasingly rapid killing via NK cell ADCC (Fig. 1c) and CDC (Fig. 1d) with increasing anti-HLA-A2 concentrations, iECs^{CD64} were fully protected, and no target cell killing was observed. The anti-HLA-A2 antibody in CDC assays was added to complete human serum containing 6–16 mg ml^{-1} of total IgG, so that it had to compete with all serum IgG for target cell CD64. To assess whether this antibody protection would hold up in patients experiencing clinically relevant AMR, we identified two transplant recipients with anti-HLA-A2 mean fluorescence intensities (MFIs) >10,000 in single-antigen bead assays (Fig. 1e,f) and clinical signs of AMR of their grafts. Patient serum samples were incubated with iECs and iECs^{CD64} (Fig. 1g,h). Whereas iECs were very rapidly killed in this CDC assay, iECs^{CD64} again were completely protected without any signs of cell damage, as shown by the steady impedance for 90 hours. To next evaluate non-HLA antibody killing, we used a recombinant human IgG1 antibody against MHC class I-related sequence A (MICA)[10,11], which is constitutively expressed on ECs[12–14] (Supplementary Fig. 3a,b). We again observed that iECs were very susceptible to NK cell ADCC and CDC, whereas iECs^{CD64} were fully protected. These experiments show that high CD64 expression can protect target cells from HLA and non-HLA antibody-mediated killing.

Generation of completely immune-evasive human cells

Human *B2M*$^{-/-}$*CIITA*$^{-/-}$CD47$^+$ (HIP) iECs[6] (Fig. 2a) are naturally protected from HLA antibodies given their lack of HLA class I and II expression. To confirm that, human iECs and human HIP iECs (both HLA-A2*02:01) were incubated with serum from two more transplant recipients with high anti-HLA-A2 MFIs and clinical signs of AMR (Fig. 2b). We saw CDC killing of iECs but not of HIP iECs. The killing was faster in the serum with higher anti-HLA-A2 MFI levels (Fig. 2c). The non-HLA epitope MICA is constitutively expressed on human HIP iECs (Fig. 2d), which leaves them susceptible to anti-MICA antibodies. We then generated CD64-expressing HIP iECs (HIP iECs^{CD64}), which were able to capture human IgG1 F_c in vitro (Fig. 2e,f). As expected, HIP iECs underwent increasingly rapid NK cell ADCC and CDC (Fig. 2g,h) with increasing concentrations of the humanized IgG1 anti-MICA antibody. Human HIP iECs^{CD64} were completely resistant against anti-MICA ADCC and CDC. Because both HIP iECs and HIP iECs^{CD64} were also positive for the rhesus D blood type antigen, ADCC and CDC assays were performed with a humanized IgG1 anti-Rh(D) antibody (Supplementary Fig. 4a,b). Whereas HIP iECs were killed in both assays, HIP iECs^{CD64} were resistant against anti-Rh(D) cytotoxicity. We next tested the binding affinities of IgG isotypes and found that CD64 shows high affinity to monomeric IgG1, IgG3 and IgG4 (Supplementary Fig. 3c,d). Although IgG1 is the most relevant antibody isotype in solid organ AMR, other isotypes have been documented[15]. Kidney transplant patients with donor-specific antibodies experiencing AMR were shown to predominantly have complement-fixing IgG1 and IgG3 for HLA and non-HLA antibodies[16–18]. In a clinical setting, CD64 overexpression should thus protect from the vast majority of human IgG.

We next aimed to verify antibody evasiveness with the highly cytotoxic human anti-CD52 IgG1 alemtuzumab and generated HIP iECs^{CD52} and HIP iECs^{CD52,CD64} that express its CD52 target (Fig. 3a,b). In vitro ADCC and CDC assays with alemtuzumab and allogeneic human NK cells confirmed the high cytotoxicity of alemtuzumab, already killing human HIP iECs^{CD52} at 0.0001 µg ml^{-1} (Fig. 3c,d). Human HIP iECs^{CD52,CD64} on the other side were resistant against ADCC and CDC, thus withstanding 100,000-times higher alemtuzumab concentrations. In an NSG mouse in vivo killing assay, 5 million HIP iECs^{CD52} and HIP iECs^{CD52,CD64} with different fluorescence labels were simultaneously injected intraperitoneally together with 100 million allogeneic human NK cells or macrophages and alemtuzumab (Supplementary Fig. 5a). After 48 hours, the peritoneal cells were recovered, and we saw that, with increasing alemtuzumab concentrations, we almost exclusively

https://doi.org/10.1038/s41587-022-01540-7

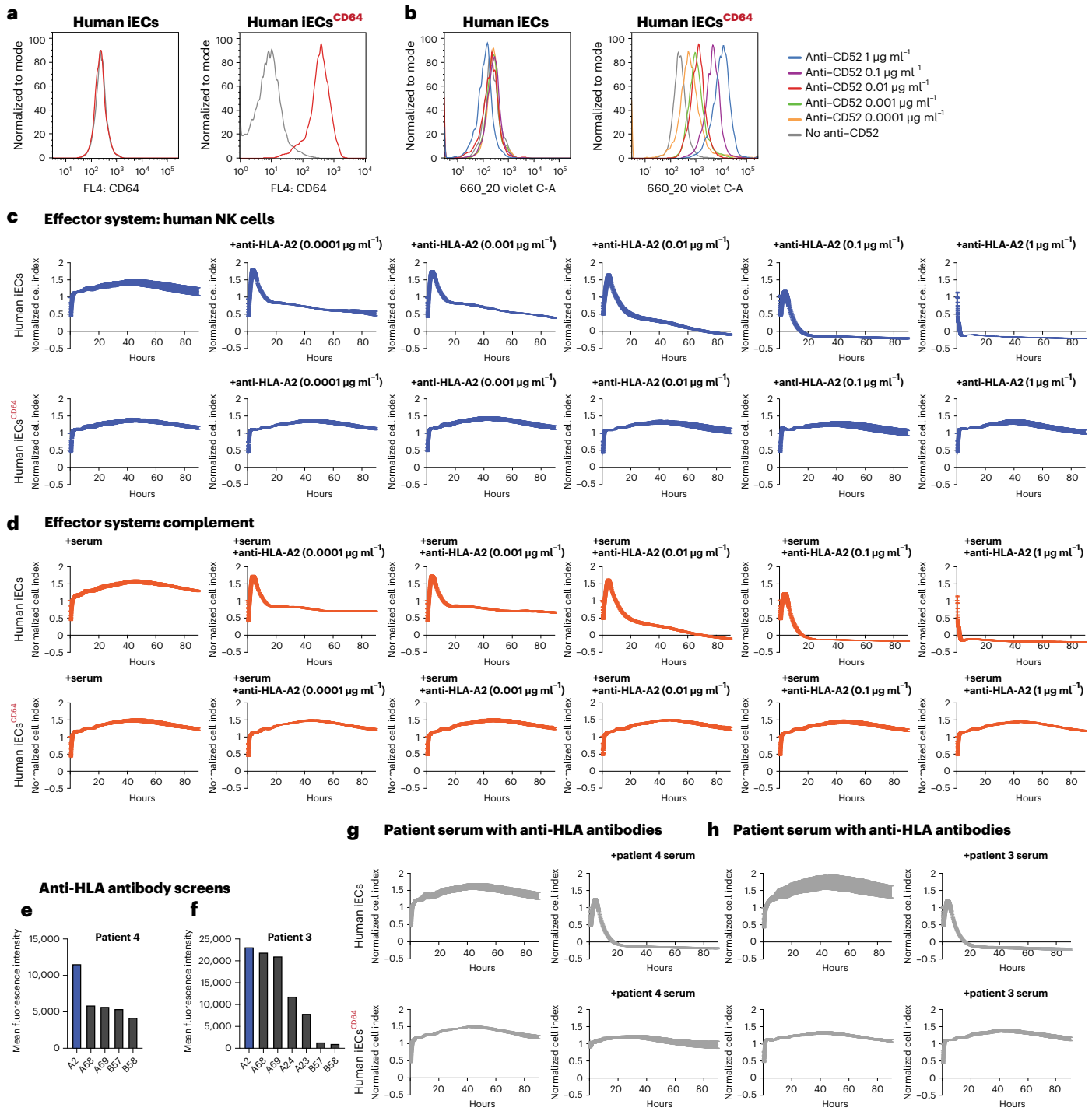

Fig. 1 | Capturing of IgG F_c protects iECs from HLA antibody-mediated killing. a, Flow cytometry histograms for CD64 expression on human iECs and iECs^{CD64} (representative graph of two independent experiments). **b**, Flow cytometry histograms for the binding of free IgG1 F_c (anti-CD52, alemtuzumab; representative graph of two independent experiments). **c**,**d**, Human iECs and iECs^{CD64} were challenged in impedance NK cell ADCC (**c**) and CDC (**d**) assays with different concentrations of an anti-HLA-A2 IgG1 antibody (mean ± s.d.; three independent replicates per group and timepoint). **e**,**f**, Single antigen bead assay results for HLA class I and II antibodies in transplant recipients 4 (**e**) and 3 (**f**) experiencing AMR. **g**,**h**, Human iECs and iECs^{CD64} were incubated with serum from patient 4 (**g**) and patient 3 (**h**) in impedance CDC assays (mean ± s.d.; three independent replicates per group and timepoint).

recovered HIP iECs^{CD52,CD64}, whereas HIP iECs^{CD52} had vanished (Supplementary Fig. 5b,c). We next assessed cell survival in an NSG mouse in vivo ADCC killing assay using BLI. A total of 5×10^4 HIP iECs^{CD52} or HIP iECs^{CD52,CD64} were injected subcutaneously with 1 million human NK cells with or without alemtuzumab (Fig. 3e). Both cell populations showed consistent survival when no antibody was added. With anti-CD52 administered at 1-mg doses on days 0, 1 and 2, HIP iECs^{CD52} were expeditiously rejected (Fig. 3f). The survival of HIP iECs^{CD52,CD64}, in contrast, remained completely unaffected (Fig. 3g). Together, these data show that CD64 expression is highly effective to prevent HIP iEC killing in vitro and in vivo by various non-HLA antibodies.

https://doi.org/10.1038/s41587-022-01540-7

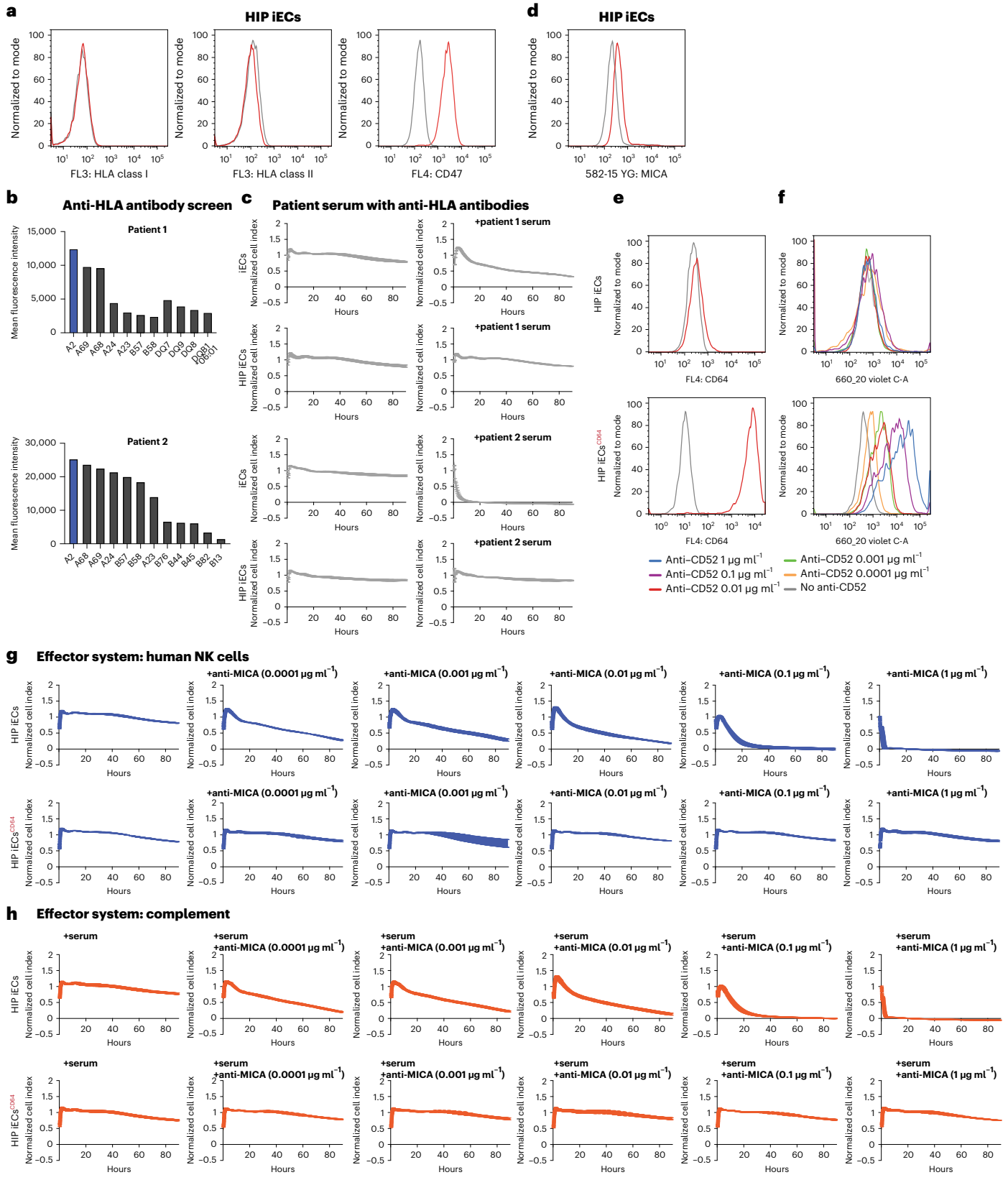

Fig. 2 | Completely immune-evasive human HIP iECs^{CD64}. **a**, The HIP immune phenotype of HLA class I and II deficiency and CD47 overexpression was confirmed in flow cytometry (representative graph of two independent experiments). **b**, Single antigen bead assay results for HLA class I and II antibodies in transplant recipients 1 and 2 experiencing AMR. **c**, Human iECs and HIP iECs were incubated with serum from both patients in impedance CDC assays (mean ± s.d.; three independent replicates per group and timepoint). **d**, Flow cytometry histogram for MICA expression on human HIP iECs (representative graph of two independent experiments). **e**, Flow cytometry histograms for CD64 expression on human HIP iECs and HIP iECs^{CD64} (representative graph of two independent experiments). **f**, Flow cytometry histograms for the binding of free IgG1 F_c (anti-CD52, alemtuzumab; representative graph of two independent experiments). **g**,**h**, Human HIP iECs and HIP iECs^{CD64} were challenged in impedance NK cell ADCC (**g**) and CDC (**h**) assays with different concentrations of an anti-MICA IgG1 antibody (mean ± s.d.; three independent replicates per group and timepoint).

https://doi.org/10.1038/s41587-022-01540-7

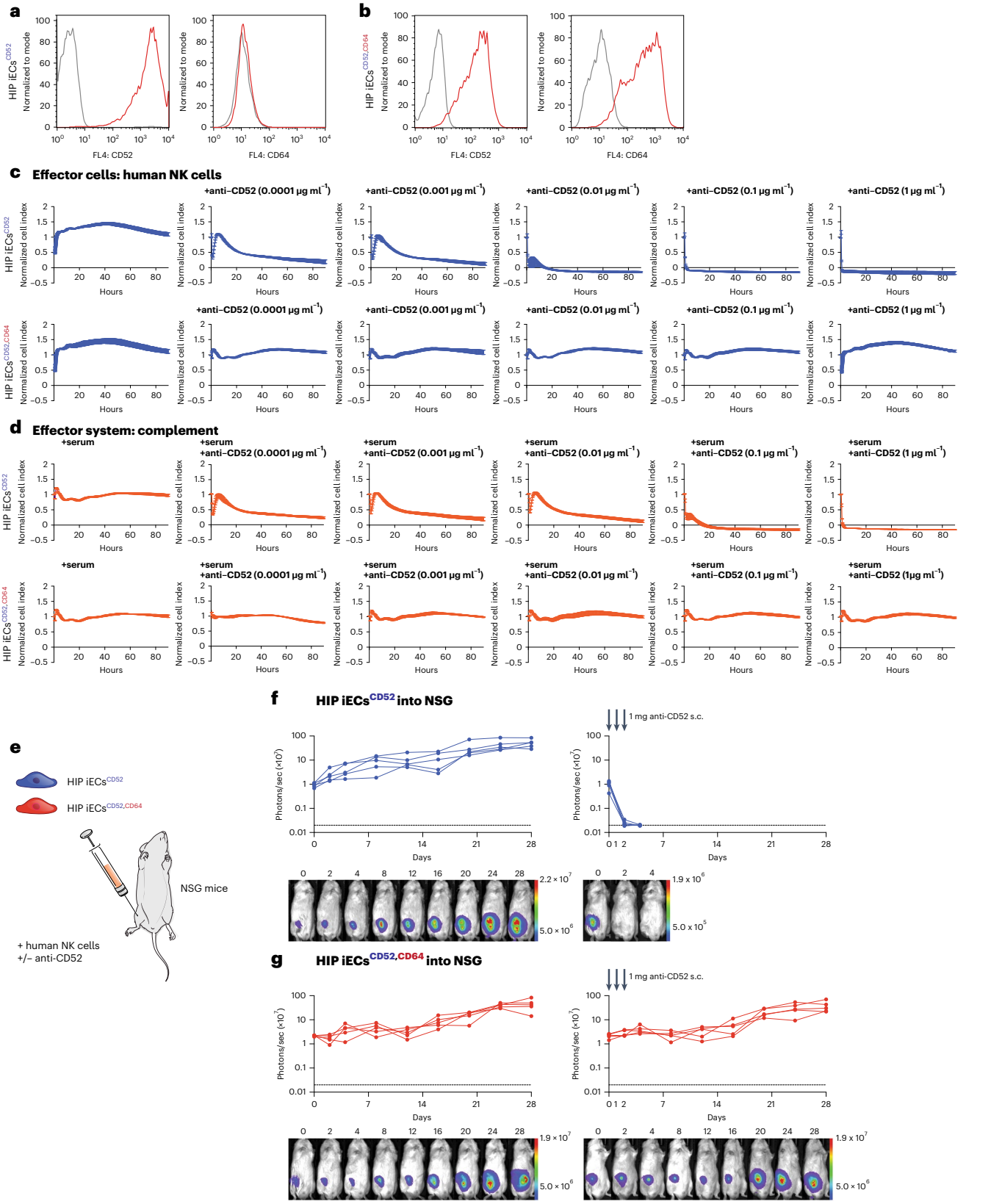

Fig. 3 | CD64 expression protects human HIP iECs^{CD52,CD64} from non-HLA antibody killing in vitro and in vivo. a, Flow cytometry histograms for CD52 and CD64 expression on human HIP iECs^{CD52} (representative graphs of two independent experiments). **b**, Flow cytometry histograms for CD52 and CD64 expression on human HIP iECs^{CD52,CD64} (representative graphs of two independent experiments). **c**,**d**, Human HIP iECs^{CD52} and HIP iECs^{CD52,CD64} were challenged in impedance NK cell ADCC (**c**) and CDC (**d**) assays with different concentrations of an anti-CD52 IgG1 antibody (mean ± s.d.; three independent replicates per group and timepoint). **e**, 5×10^4 HIP iECs^{CD52} or HIP iECs^{CD52,CD64} were injected subcutaneously into NSG mice with 10^6 human NK cells. Some groups received three subcutaneous doses of alemtuzumab 1 mg on days 0, 1 and 2. **f**,**g**, BLI signals of HIP iECs^{CD52} (**f**) and HIP iECs^{CD52,CD64} (**g**) were followed (all individual mice were plotted, and BLI pictures of one representative mouse per group are shown). s.c., subcutaneous.

https://doi.org/10.1038/s41587-022-01540-7

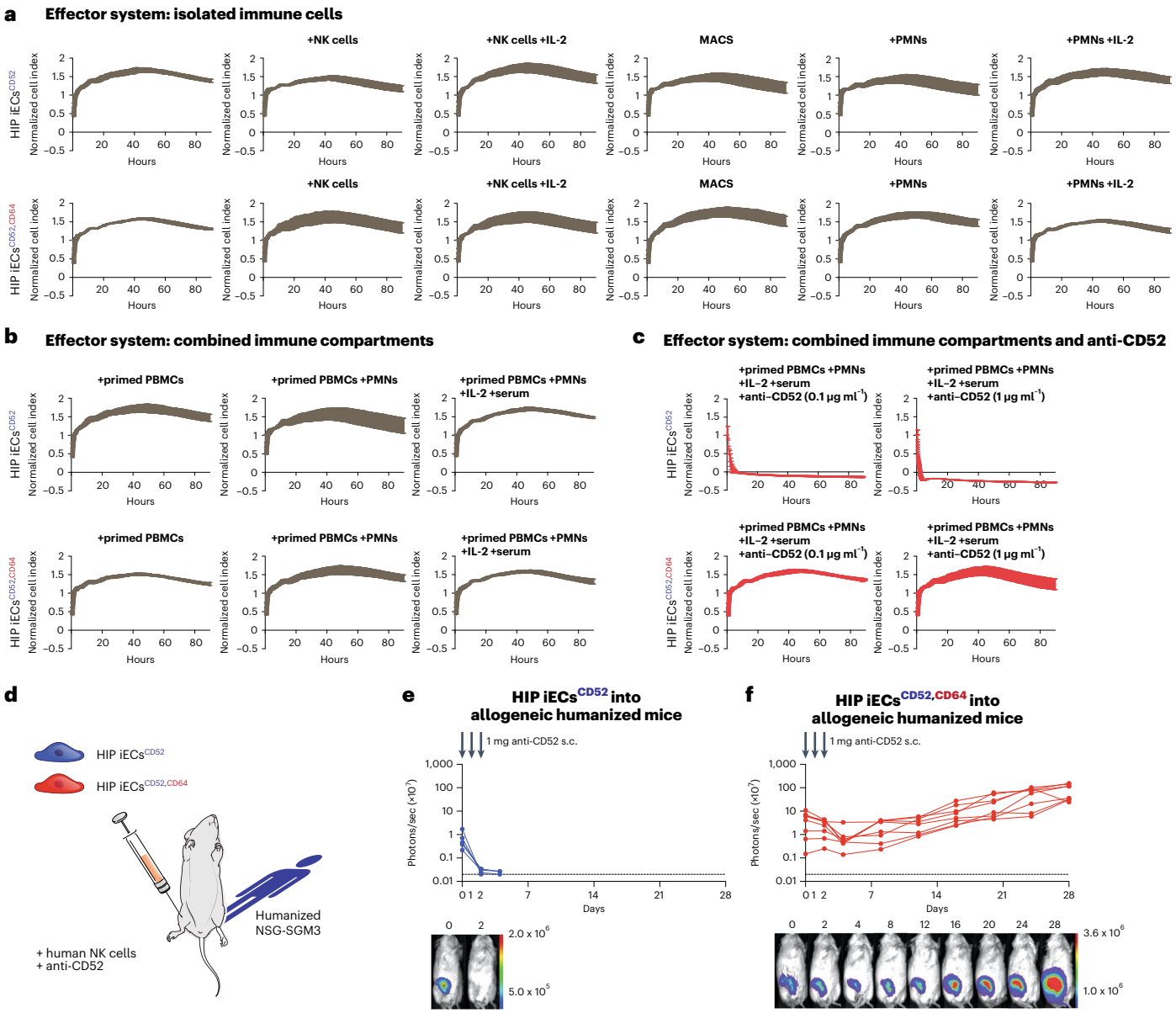

Fig. 4 | Human HIP iECs^{CD52,CD64} evade all cellular and antibody-mediated immune attacks. a, Human HIP iECs^{CD52} and HIP iECs^{CD52,CD64} were challenged with isolated allogeneic innate immune cells. Allogeneic NK cells with or without IL-2, allogeneic macrophages or allogeneic PMN cells with or without IL-2 were used. **b**, Human HIP iECs^{CD52} and HIP iECs^{CD52,CD64} were challenged with primed allogeneic PBMCs after they underwent 10 days of in vitro stimulation with the target cells. Then, PMNs and serum were added to combine all immune compartments of the peripheral blood in this assay. **c**, Human HIP iECs^{CD52} and HIP iECs^{CD52,CD64} were challenged with all immune compartments of the peripheral blood while adding anti-CD52 to enable ADCC and CDC. All graphs show mean ± s.d. and three independent replicates per group and timepoint. **d**, 5×10^4 HIP iECs^{CD52} or HIP iECs^{CD52,CD64} were injected subcutaneously into humanized mice with 10^6 human NK cells. Both groups received three subcutaneous doses of anti-CD52 IgG1 (alemtuzumab) 1 mg on days 0, 1 and 2. **e**,**f**, BLI signals of HIP iECs^{CD52} (**f**) and HIP iECs^{CD52,CD64} (**g**) were followed (all individual mice were plotted, and BLI pictures of one representative mouse per group are shown). s.c., subcutaneous.

Finally, HIP iECs^{CD52,CD64} were exposed to increasingly harsh allogeneic immune environments to challenge their complete immune-evasiveness. Killing assays were first performed with only allogeneic NK cells, macrophages or polymorphonuclear (PMN) cells (Fig. 4a). Then, the whole cellular immune compartment of peripheral blood mononuclear cells (PBMCs) underwent 10 days of in vitro priming against the target cells to activate any possible adaptive immunity and was then used for the killing assay. We then added two more immune compartments, PMNs and complement-rich serum (Fig. 4b). The fact that the survival of both HIP iECs^{CD52} and HIP iECs^{CD52,CD64} remained unaffected confirms the reliability of the HIP technology to escape all cellular immunity. However, when anti-CD52 was added to enable ADCC and CDC, then HIP iECs^{CD52} were rapidly killed (Fig. 4c). HIP iECs^{CD52,CD64} were resistant against both allogeneic cellular and antibody-mediated killing.

For in vivo testing of complete immune-evasiveness, 5×10^4 HIP iECs^{CD52} or HIP iECs^{CD52,CD64} were injected subcutaneously into humanized NSG-SGM3 mice reconstituted with allogeneic CD34$^+$ human hematopoietic stem cells. The cellular grafts were mixed with 1 million human NK cells before injection, and 1-mg doses of alemtuzumab were administered on days 0, 1 and 2 (Fig. 4d). All HIP iECs^{CD52} grafts were quickly rejected (Fig. 4e), whereas all HIP iECs^{CD52,CD64} grafts survived (Fig. 4f). Only HIP iECs^{CD52,CD64} were completely resistant against all forms of allogeneic cellular and antibody-mediated immune attacks.

Mechanistic features of F_c capturing

Macrophages constitutively express CD64 and, thus, have some intrinsic protection against ADCC and CDC in the presence of anti-CD52 (Supplementary Fig. 6). When CD64 was knocked down using short hairpin RNA (shRNA), macrophages lost their protection. To test whether a second antibody would displace anti-CD52 IgG1 from CD64 and break the antibody-evasiveness of HIP iECs^{CD52,CD64}, alemtuzumab had to compete with rituximab, a human IgG1 antibody against CD20, an epitope not expressed on iECs. (Supplementary Fig. 7). NK ADCC assays and CDC assays, however, confirmed the robustness of antibody protection, which could not be broken through competitive F_c displacement, even when alemtuzumab was given later. When FcγRIIB, the F_c receptor with the lowest IgG1 binding affinity, was used instead of CD64, the antibody protection was several orders of magnitudes lower than that for CD64 (Supplementary Fig. 8a–d). In further support of the notion that the protection against antibodies was dependent on the ability of CD64 to capture IgG F_c, we found that HIP iECs^{CD52,CD64} were resistant against anti-CD52 human IgG1 but susceptible to an anti-CD52 mouse IgG2b, a subclass not binding to CD64[19] (Supplementary Fig. 8e,f). Antibody protection through CD64 was saturable, with low surface expression failing to protect against higher antibody concentrations (Supplementary Fig. 9a–d). Mechanistically, captured IgG1 bound to and occupied their target epitopes and made them unavailable for antibodies with lower F_c affinity to CD64 (Supplementary Fig. 9e), without affecting internalization of antibody–epitope complexes (Supplementary Fig. 9f–h). The next experiments were designed to reveal F_c and F_{ab} binding patterns of competitive antibodies. HIP cells were incubated with anti-CD20 IgG1 at fixed dose and increasing doses of anti-CD52 IgG1. When competing for CD64 on HIP iECs^{CD64}, anti-CD52 binding increased in a concentration-dependent manner at the expense of anti-CD20 binding (Supplementary Fig. 10a,b). On HIP iECs^{CD52,CD64}, the overall binding of anti-CD52 was enhanced and the reduction of anti-CD20 further facilitated with a significant interactive effect that was larger in magnitude (Supplementary Fig. 10c,d). Anti-CD20 showed negligible binding to HIP iECs^{CD52,FcγRIIB} and remained unaffected by anti-CD52 binding (Supplementary Fig. 10e,f), and the interactive effect was not significant. In contrast, when competing with a human IgG1 F_c fragment for CD64, the binding of anti-CD20 on HIP iECs^{CD64} and HIP iECs^{CD52,CD64} was qualitatively equivalent (Supplementary Fig. 11). Next, two anti-CD52 antibodies with cytotoxic properties in CDC assays (Supplementary Fig. 12a, Supplementary Fig. 8f and Fig. 3d) were competing for HIP iECs^{CD52,CD64} binding in mouse serum. Only the human IgG1, but not the mouse IgG2b, could additionally ligate CD64. When mainly the mouse IgG2b was bound, we observed rapid target cell killing. When the mouse IgG2b was diminished with increasing concentrations of the human IgG1, the killing gradually slowed down and ceased at the high end (Supplementary Fig. 12b,c). Together, these results show how a favorable binding pattern of cytotoxic antibodies with high F_c affinity to CD64 establishes protection even in the presence of competing antibodies.

To assess whether antibody capturing also affects $CD8^+$ T cell cytotoxicity, we primed PBMCs from an HLA-$A2^-$ donor against HLA-$A2^+$ iECs in vitro (Supplementary Fig. 12d). Primed $CD8^+$ T cells killed both iECs and iECs^{CD64} with similar kinetics (Supplementary Fig. 12e). However, when cytotoxic anti-HLA-A2 antibodies were added, only iECs were killed more quickly. iECs^{CD64} were protected from $CD8^+$ T cell ADCC, even after the target cells were incubated with anti-CD20 for 30 minutes to saturate CD64. Overall, these results confirmed that F_c capturing also protects against $CD8^+$ T cell ADCC.

Next, applications of this technology were explored. Because CD64 downstream signaling after F_c ligation could alter the physiology of some engineered cell types, we used a truncated form of CD64 lacking its intracellular tail for all the following translational applications. Expression of truncated CD64 (CD64t) was found to be similarly effective in preventing NK cell and $CD8^+$ T cell ADCC and CDC as full-length CD64 (Supplementary Fig. 13).

Engineered human thyroid cells evade autoimmune antibody killing

Hashimoto's thyroiditis is a prototypic disease in which cytotoxic autoantibodies lead to the destruction of thyroid tissue. Anti-thyroid peroxidase (TPO) antibodies, primarily of IgG1 subclass, are present at high concentrations in 90% of patients[20,21], have been shown to mediate both ADCC[22–24] and CDC[25,26] and diminish the function of the thyroid gland[27]. Thyroid epithelial cells (epiCs) resistant to TPO antibodies would have a much better chance to survive and re-establish organ function if transplanted into hypothyroid patients. Functionally immortalized human thyroid epithelial cells were first transduced to enhance their expression of TPO, because cells in culture tend to downregulate its expression (Supplementary Fig. 14a). Then, epiCs were transduced to express CD64t, which was effective in binding free human IgG1 F_c (Supplementary Fig. 14b). Both thyroid epiCs^{TPO} and epiCs^{TPO,CD64t} produced thyroxine irrespective of the presence of IgG1 antibodies (Supplementary Fig. 14c). A humanized anti-TPO IgG1 antibody was effective in killing thyroid epiCs^{TPO} in ADCC and CDC assays, whereas thyroid epiCs^{TPO,CD64t} were fully protected (Fig. 5a,b). Serum samples from three patients with Hashimoto's thyroiditis and anti-TPO antibody titers 21-fold, 26.3-fold and 29.6-fold the upper level of normal rapidly killed thyroid epiCs^{TPO} in CDC assays (Fig. 5c–e). Thyroid epiCs^{TPO,CD64t} were completely protected from killing in patient serum and, thus, withstood clinically relevant autoimmune conditions. NSG recipients were subcutaneously injected with 5×10^4 epiCs^{TPO} or epiCs^{TPO,CD64t}, 1 million human NK cells and 1-mg doses of anti-TPO on days 0, 1 and 2 (Fig. 5f). All epiCs^{TPO} grafts vanished quickly (Fig. 5g), whereas all epiCs^{TPO,CD64t} grafts survived (Fig. 5h).

Engineered human beta cells evade HLA antibody killing

Type 1 diabetes mellitus (T1DM) is another autoimmune disease, which is T cell mediated with an accompanying antibody response. We aimed to test whether CD64t expression can make them resistant against HLA antibody killing. Human iPSC-derived beta cells transduced to express CD64t (Supplementary Fig. 15a) were able to capture and bind free IgG F_c (Supplementary Fig. 15b). Both beta cells and beta cells^{CD64t} showed intact glucose sensing and insulin production irrespective of the presence of antibodies (Supplementary Fig. 15c). HLA-A2-expressing beta cells were killed increasingly quickly with increasing anti-HLA-A2 IgG1 antibody concentrations in ADCC and CDC assays (Supplementary Fig. 15d,e). Beta cells^{CD64t}, however, were completely resistant against HLA antibody-mediated killing. We then subcutaneously injected NSG mice with 5×10^4 human beta cells or beta cells^{CD64t} together with 1 million human NK cells. Three 1-mg doses of anti-HLA-A2 IgG1 were subcutaneously injected on days 0, 1 and 2 (Supplementary Fig. 15f). All beta cell grafts vanished within 2 days, whereas all beta cell^{CD64t} grafts defied antibody-mediated killing and paralleled the survival of beta cells without antibody challenge (Supplementary Fig. 15g–i).

Engineered human CAR T cells evade HLA and non-HLA antibody killing

Clinical CAR T cell therapy induces an antibody response, which is even more pronounced in patients with solid tumors. To test whether we can engineer antibody protection into CAR T cells, we transduced human T cells to express a CD19 scFv-4-1BB-CD3ζ construct with or without additional CD64t expression (Fig. 6a). CAR T^{CD64t} cells were able to capture and bind free IgG1 F_c (Fig. 6b). The killing efficacy of CAR T, CAR T^{CD64t} and regular T cells was assessed against $CD19^+$ Nalm6 target cells. Whereas control T cells showed no killing, both CAR T and CAR T^{CD64t} cells were equally effective killers across a wide range of effector cell-to-target cell ratios (Fig. 6c). Furthermore, the tumor killing capacity of CAR T^{CD64t} cells was not affected by the presence of F_c-bound antibodies (Fig. 6d). ADCC and CDC assays with cytotoxic antibodies against an HLA epitope (HLA-A2), non-HLA epitopes (CD52

https://doi.org/10.1038/s41587-022-01540-7

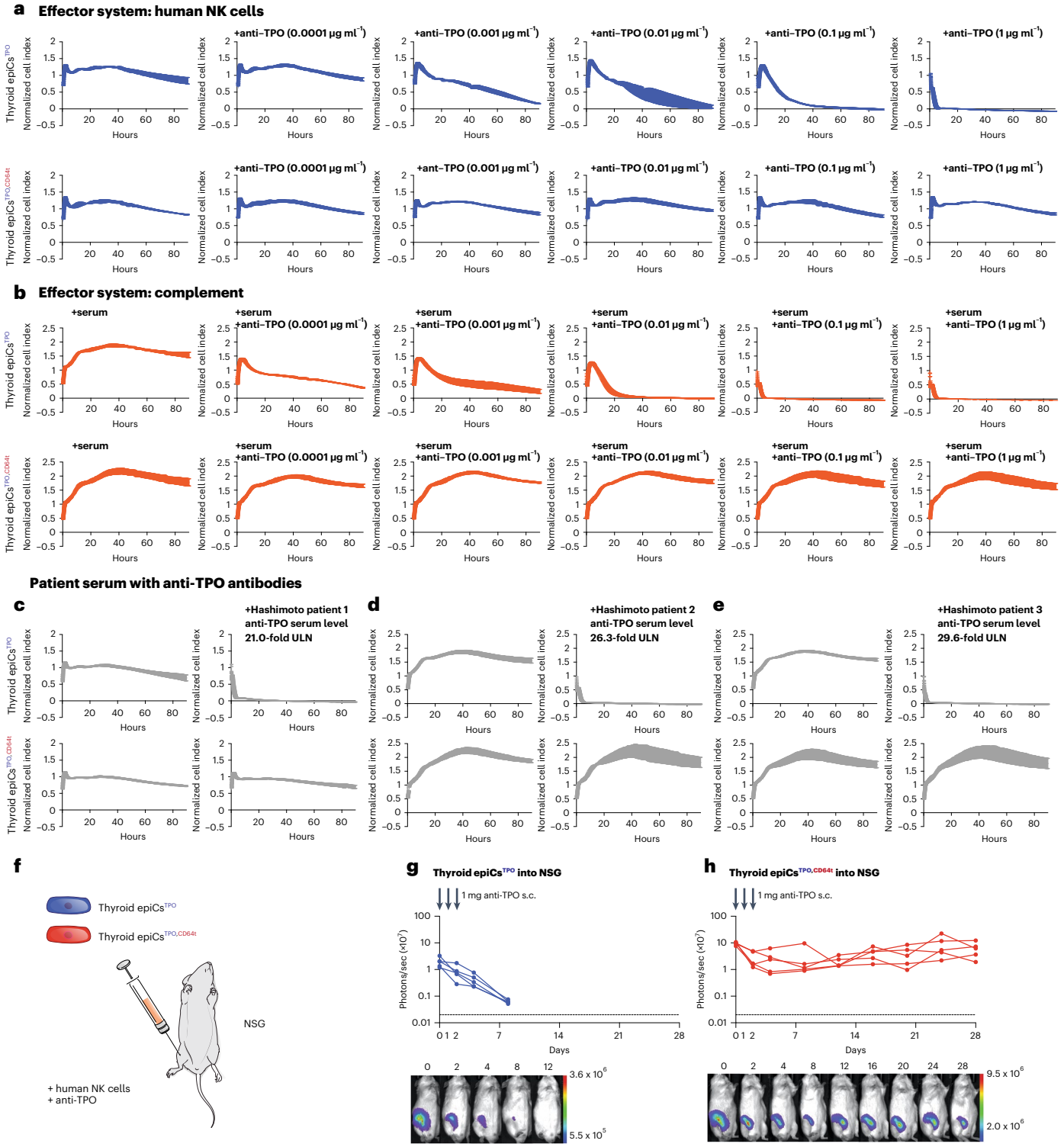

Fig. 5 | Human thyroid epiCs^{TPO,CD64t} are protected from antibody-mediated killing. a,**b**, Human thyroid epiCs^{TPO} and epiCs^{TPO,CD64t} were challenged in impedance NK cell ADCC (**a**) and CDC (**b**) assays with different concentrations of an anti-TPO IgG1 antibody (mean ± s.d.; three independent replicates per group and timepoint). **c**–**e**, Human thyroid epiCs^{TPO} and epiCs^{TPO,CD64t} were incubated with serum from Hashimoto's patients 1 (**c**), 2 (**d**) and 3 (**e**) in impedance CDC assays (mean ± s.d.; three independent replicates per group and timepoint). ULN, upper limit of normal. **f**, 5×10^4 human thyroid epiCs^{TPO} or epiCs^{TPO,CD64t} were injected subcutaneously into NSG mice with 10^6 human NK cells. Both groups received three subcutaneous doses of anti-TPO IgG1 1 mg on days 0, 1 and 2. **g**,**h**, BLI signals of thyroid epiCs^{TPO} (**g**) and epiCs^{TPO,CD64t} (**h**) were followed (all individual mice were plotted, and BLI pictures of one representative mouse per group are shown). s.c., subcutaneous.

and CD3), a blood type antigen (Rh(D)) and the CAR receptor (anti-CD19 scFv) were performed, and the CAR T cells were killed in all assays (Fig. 6e,f). CAR T^{CD64t} cells, however, were able to evade antibody-mediated killing with all five antibodies in all assays. CD64t expression does not affect the cytotoxicity of human CAR T cells but makes them resistant against antibodies irrespective of their specificities.

https://doi.org/10.1038/s41587-022-01540-7

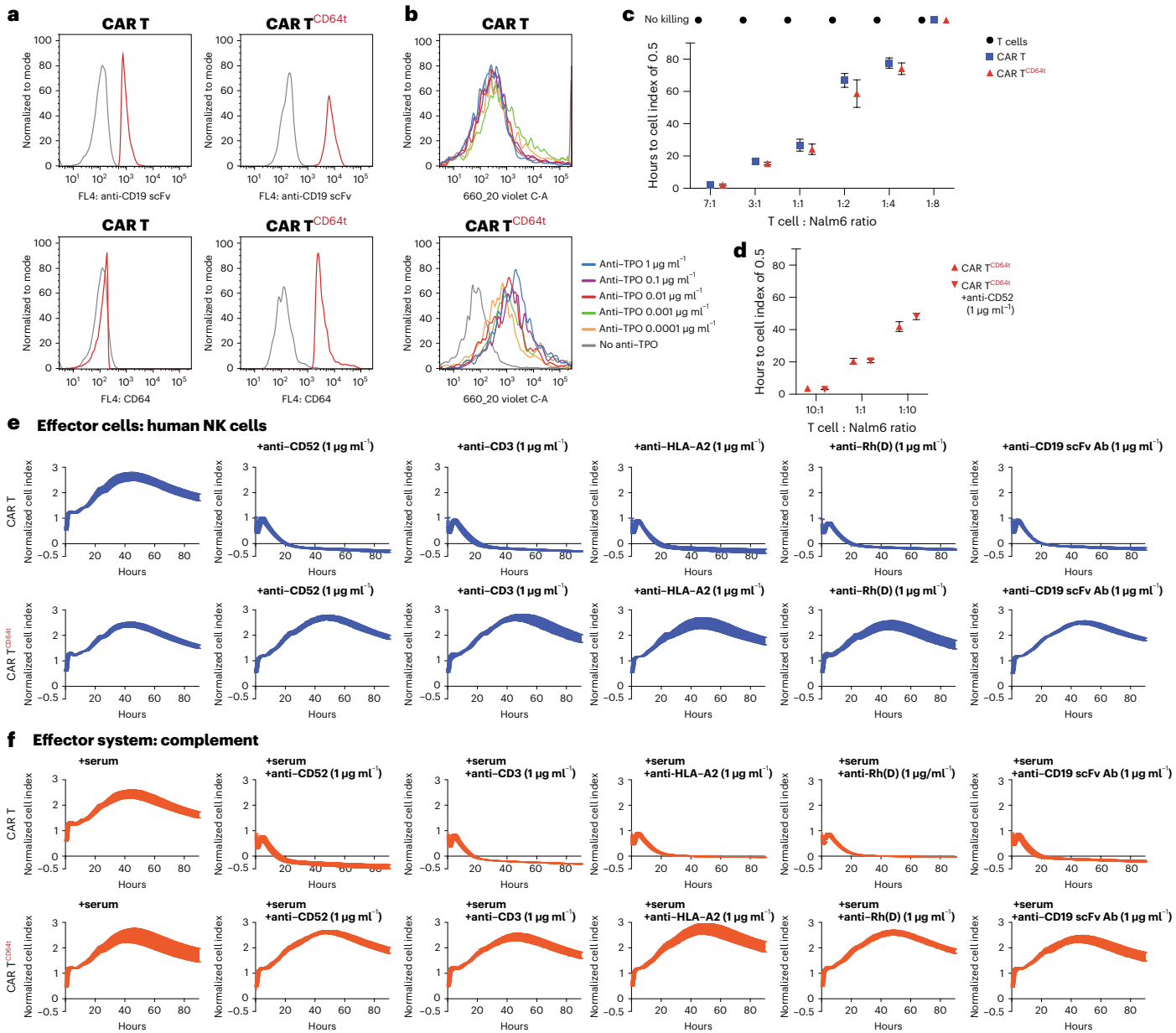

Fig. 6 | Human CAR T^{CD64t} cells are protected from antibody-mediated killing. **a**, Flow cytometry histograms for anti-CD19 scFv and CD64t expression on human CAR T and CAR T^{CD64t} cells (representative graphs of two independent experiments). **b**, Flow cytometry histograms for the binding of free IgG1 F_c (anti-TPO IgG1; representative graph of two independent experiments). **c**, The kinetics of Nalm6 target cell killing by T cells, CAR T cells and CAR T^{CD64t} cells is expressed as hours that it takes for the cell index to drop from 1 to 0.5. Different T cell-to-Nalm6 ratios are shown (mean ± s.d.; three independent replicates per group and timepoint). **d**, The kinetics of Nalm6 target cell killing by CAR T^{CD64t} in the presence and absence of 1 µg ml^{-1} of anti-CD52 is expressed as hours that it takes for the cell index to drop from 1 to 0.5. Different CAR T cell-to-Nalm6 ratios are shown (mean ± s.d.; three independent replicates per group and timepoint). **e**,**f**, Human CAR T and CAR T^{CD64t} cells were challenged in impedance NK cell ADCC (**e**) and CDC (**f**) assays with antibodies against HLA (HLA-A2), non-HLA (CD52 and CD3), rhesus blood type antigen D (Rh(D)) and the CAR (anti-CD19 scFv) at 1 µg ml^{-1} (mean ± s.d.; three independent replicates per group and timepoint).

Discussion

Immune rejection presents the principal hurdle for the success of cell therapeutics, and much effort is currently devoted to developing universal allogeneic off-the-shelf cells that evade cellular rejection[28–30]. Such gene-edited HIP cells, however, remain susceptible to antibody killing directed against non-HLA epitopes, cell-type-specific autoantigens as well as xenogeneic[31] or synthetic constructs[32] in engineered cells and viral products from the transduction process[33,34]. Cytotoxic antibodies can be pre-existing or treatment induced[35] and jeopardize the persistence and efficacy of the cell therapeutics.

We aimed to expand the HIP concept to antibody resistance using non-immunogenic components. Microbial IgG-degrading enzymes have been administered systemically to deplete total IgG and HLA antibodies in highly sensitized patients before kidney transplantation[36]. More recently, these endopeptidases were shown to cleave IgG bound to target cells[37]. However, pre-existing antibodies against these bacterial enzymes are prevalent in the healthy population[38], spike during streptococcal infections[39,40] and might themselves add unwanted immunogenicity. We have shown that human CD64 and its truncated form CD64t, which are non-immunogenic, have high affinity

for IgG[41] and protect very effective against antibody killing in several translationally relevant cell types.

Applications for this technology include regenerative cell therapeutics, especially for diseases with an underlying autoimmune component in which antibodies are present that would destroy the transplanted cells[42]. Regenerative cell therapeutics would be destroyed similarly to the native cells if autoimmunity would not be circumvented[42]. Supporting this notion, we show that engineered epiCs^{TPO,CD64t} were protected against clinically relevant anti-TPO killing. The most advanced stem-cell-derived pancreatic islet cells prepared for clinical trials in patients with T1DM are currently produced from embryonic stem cells (ESCs)[43] and, thus, are transplanted across an HLA mismatch. Currently, such ESC-derived beta cells are transplanted in immunoprotective encapsulation devices[44] or with immunosuppression[45,46]. We found that forced overexpression of CD64t on human beta cells was sufficient to protect them from anti-HLA ADCC and CDC.

Most success in CAR T cell therapy has been achieved with B cell neoplasms in which patients are treated with lymphocytotoxic drugs, and the CAR T cells directly target the B cell source of antibody production[47], although antibody induction is still regularly observed[48]. An antibody response against a second infusion of CAR T cells has been documented in four out of 12 patients studied, and none of these patients showed expansion of CAR T cells in their blood[37]. The expression of CD64t on CAR T cells makes them resistant against anti-CAR T cell antibodies without affecting their specific killing capacity. Because early immune clearance is even more common in non-B cell cancer, CAR T^{CD64t} may be more efficient for these indications. The capturing of cytotoxic IgG F_c reliably builds protection against antibodies in several cell types and could further advance the immune-evasion concept for allogeneic regenerative and immune-oncology cell therapeutics.

Online content

Any methods, additional references, Nature Research reporting summaries, source data, extended data, supplementary information, acknowledgements, peer review information; details of author contributions and competing interests; and statements of data and code availability are available at https://doi.org/10.1038/s41587-022-01540-7.

References

1. Loupy, A. & Lefaucheur, C. Antibody-mediated rejection of solid-organ allografts. *N. Engl. J. Med.* **379**, 1150–1160 (2018).
2. Menasche, P. et al. Human embryonic stem cell-derived cardiac progenitors for severe heart failure treatment: first clinical case report. *Eur. Heart J.* **36**, 2011–2017 (2015).
3. Panes, J. et al. Expanded allogeneic adipose-derived mesenchymal stem cells (Cx601) for complex perianal fistulas in Crohn's disease: a phase 3 randomised, double-blind controlled trial. *Lancet* **388**, 1281–1290 (2016).
4. Skyler, J. S., Fonseca, V. A., Segal, K. R., Rosenstock, J. & Investigators, M.-D. Allogeneic mesenchymal precursor cells in type 2 diabetes: a randomized, placebo-controlled, dose-escalation safety and tolerability pilot study. *Diabetes Care* **38**, 1742–1749 (2015).
5. Hege, K. M. et al. Safety, tumor trafficking and immunogenicity of chimeric antigen receptor (CAR)-T cells specific for TAG-72 in colorectal cancer. *J. Immunother. Cancer* **5**, 22 (2017).
6. Deuse, T. et al. Hypoimmunogenic derivatives of induced pluripotent stem cells evade immune rejection in fully immunocompetent allogeneic recipients. *Nat. Biotechnol.* **37**, 252–258 (2019).
7. Deuse, T. et al. The SIRPα-CD47 immune checkpoint in NK cells. *J. Exp. Med.* **218**, e20200839 (2021).
8. Renard, V. et al. Normal development and function of natural killer cells in CD3 epsilon delta 5/delta 5 mutant mice. *Proc. Natl Acad. Sci. USA* **92**, 7545–7549 (1995).
9. Watkins, N. A., Brown, C., Hurd, C., Navarrete, C. & Ouwehand, W. H. The isolation and characterisation of human monoclonal HLA-A2 antibodies from an immune V gene phage display library. *Tissue Antigens* **55**, 219–228 (2000).
10. Shiina, T., Hosomichi, K., Inoko, H. & Kulski, J. K. The HLA genomic loci map: expression, interaction, diversity and disease. *J. Hum. Genet.* **54**, 15–39 (2009).
11. Leelayuwat, C., Townend, D. C., Degli-Esposti, M. A., Abraham, L. J. & Dawkins, R. L. A new polymorphic and multicopy MHC gene family related to nonmammalian class I. *Immunogenetics* **40**, 339–351 (1994).
12. Zou, Y., Stastny, P., Susal, C., Dohler, B. & Opelz, G. Antibodies against MICA antigens and kidney-transplant rejection. *N. Engl. J. Med.* **357**, 1293–1300 (2007).
13. Suarez-Alvarez, B. et al. The relationship of anti-MICA antibodies and MICA expression with heart allograft rejection. *Am. J. Transplant.* **7**, 1842–1848 (2007).
14. Angaswamy, N. et al. Development of antibodies to human leukocyte antigen precedes development of antibodies to major histocompatibility class I-related chain A and are significantly associated with development of chronic rejection after human lung transplantation. *Hum. Immunol.* **71**, 560–565 (2010).
15. Valenzuela, N. M. & Reed, E. F. Antibody-mediated rejection across solid organ transplants: manifestations, mechanisms, and therapies. *J. Clin. Invest.* **127**, 2492–2504 (2017).
16. Honger, G. et al. Pretransplant IgG subclasses of donor-specific human leukocyte antigen antibodies and development of antibody-mediated rejection. *Transplantation* **92**, 41–47 (2011).
17. Arnold, M. L. et al. Donor-specific HLA antibodies: evaluating the risk for graft loss in renal transplant recipients with isotype switch from complement fixing IgG1/IgG3 to noncomplement fixing IgG2/IgG4 anti-HLA alloantibodies. *Transpl. Int.* **27**, 253–261 (2014).
18. Dragun, D. Agonistic antibody-triggered stimulation of angiotensin II type 1 receptor and renal allograft vascular pathology. *Nephrol. Dial. Transplant.* **22**, 1819–1822 (2007).
19. Pfefferkorn, L. C., van de Winkel, J. G. & Swink, S. L. A novel role for IgG-Fc. Transductional potentiation for human high affinity Fcγ receptor (Fcγ RI) signaling. *J. Biol. Chem.* **270**, 8164–8171 (1995).
20. Rapoport, B. & McLachlan, S. M. Thyroid autoimmunity. *J. Clin. Invest.* **108**, 1253–1259 (2001).
21. Doullay, F., Ruf, J., Codaccioni, J. L. & Carayon, P. Prevalence of autoantibodies to thyroperoxidase in patients with various thyroid and autoimmune diseases. *Autoimmunity* **9**, 237–244 (1991).
22. Bogner, U., Schleusener, H. & Wall, J. R. Antibody-dependent cell mediated cytotoxicity against human thyroid cells in Hashimoto's thyroiditis but not Graves' disease. *J. Clin. Endocrinol. Metab.* **59**, 734–738 (1984).
23. Stathatos, N. & Daniels, G. H. Autoimmune thyroid disease. *Curr. Opin. Rheumatol.* **24**, 70–75 (2012).
24. Stassi, G. & De Maria, R. Autoimmune thyroid disease: new models of cell death in autoimmunity. *Nat. Rev. Immunol.* **2**, 195–204 (2002).
25. Rebuffat, S. A., Nguyen, B., Robert, B., Castex, F. & Peraldi-Roux, S. Antithyroperoxidase antibody-dependent cytotoxicity in autoimmune thyroid disease. *J. Clin. Endocrinol. Metab.* **93**, 929–934 (2008).
26. Chiovato, L. et al. Antibodies producing complement-mediated thyroid cytotoxicity in patients with atrophic or goitrous autoimmune thyroiditis. *J. Clin. Endocrinol. Metab.* **77**, 1700–1705 (1993).
27. Pearce, E. N., Farwell, A. P. & Braverman, L. E. Thyroiditis. *N. Engl. J. Med.* **348**, 2646–2655 (2003).
28. Yoshihara, E. et al. Immune-evasive human islet-like organoids ameliorate diabetes. *Nature* **586**, 606–611 (2020).

29. Wang, B. et al. Generation of hypoimmunogenic T cells from genetically engineered allogeneic human induced pluripotent stem cells. *Nat. Biomed. Eng.* **5**, 429–440 (2021).
30. Deuse, T. et al. Hypoimmune induced pluripotent stem cell-derived cell therapeutics treat cardiovascular and pulmonary diseases in immunocompetent allogeneic mice. *Proc. Natl Acad. Sci. USA* **118**, e2022091118 (2021).
31. Klee, G. G. Human anti-mouse antibodies. *Arch. Pathol. Lab. Med.* **124**, 921–923 (2000).
32. Choe, J. H. et al. SynNotch-CAR T cells overcome challenges of specificity, heterogeneity, and persistence in treating glioblastoma. *Sci. Transl. Med.* **13**, eabe7378 (2021).
33. Lamers, C. H. et al. Immune responses to transgene and retroviral vector in patients treated with ex vivo-engineered T cells. *Blood* **117**, 72–82 (2011).
34. Jensen, M. C. et al. Antitransgene rejection responses contribute to attenuated persistence of adoptively transferred CD20/CD19-specific chimeric antigen receptor redirected T cells in humans. *Biol. Blood Marrow Transplant.* **16**, 1245–1256 (2010).
35. Wagner, D. L. et al. Immunogenicity of CAR T cells in cancer therapy. *Nat. Rev. Clin. Oncol.* **18**, 379–393 (2021).
36. Jordan, S. C. et al. IgG endopeptidase in highly sensitized patients undergoing transplantation. *N. Engl. J. Med.* **377**, 442–453 (2017).
37. Peraro, L. et al. Incorporation of bacterial immunoevasins to protect cell therapies from host antibody-mediated immune rejection. *Mol. Ther.* **29**, 3398–3409 (2021).
38. Akesson, P. et al. Low antibody levels against cell wall-attached proteins of *Streptococcus pyogenes* predispose for severe invasive disease. *J. Infect. Dis.* **189**, 797–804 (2004).
39. Lei, B. et al. Evasion of human innate and acquired immunity by a bacterial homolog of CD11b that inhibits opsonophagocytosis. *Nat. Med.* **7**, 1298–1305 (2001).
40. Okamoto, S., Tamura, Y., Terao, Y., Hamada, S. & Kawabata, S. Systemic immunization with streptococcal immunoglobulin-binding protein Sib 35 induces protective immunity against group: a *Streptococcus* challenge in mice. *Vaccine* **23**, 4852–4859 (2005).
41. Bruhns, P. et al. Specificity and affinity of human Fcγ receptors and their polymorphic variants for human IgG subclasses. *Blood* **113**, 3716–3725 (2009).
42. Hollenberg, A. N., Choi, J., Serra, M. & Kotton, D. N. Regenerative therapy for hypothyroidism: mechanisms and possibilities. *Mol. Cell. Endocrinol.* **445**, 35–41 (2017).
43. Melton, D. The promise of stem cell-derived islet replacement therapy. *Diabetologia* **64**, 1030–1036 (2021).
44. Desai, T. & Shea, L. D. Advances in islet encapsulation technologies. *Nat. Rev. Drug Discov.* **16**, 338–350 (2017).
45. Ramzy, A. et al. Implanted pluripotent stem-cell-derived pancreatic endoderm cells secrete glucose-responsive C-peptide in patients with type 1 diabetes. *Cell Stem Cell* **28**, 2047–2061 (2021).
46. Shapiro, A. M. J. et al. Insulin expression and C-peptide in type 1 diabetes subjects implanted with stem cell-derived pancreatic endoderm cells in an encapsulation device. *Cell Rep. Med.* **2**, 100466 (2021).
47. Brudno, J. N. & Kochenderfer, J. N. Chimeric antigen receptor T-cell therapies for lymphoma. *Nat. Rev. Clin. Oncol.* **15**, 31–46 (2018).
48. Till, B. G. et al. Adoptive immunotherapy for indolent non-Hodgkin lymphoma and mantle cell lymphoma using genetically modified autologous CD20-specific T cells. *Blood* **112**, 2261–2271 (2008).

Methods

Mice

C57BL/6 (C57BL/6J, B6, H2^b, 000664), Rag-1 knockout (KO) (B6.129S7-Rag1^{tm1Mom}/J, 002216) and NSG (NOD.Cg-*Prkdc*^{scid} *Il2rg*^{tm1Wjl}/SzJ, 005557) mice, 6–12 weeks old, and humanized NSG-SGM3 (NOD.Cg-*Prkdc*^{scid} *Il2rg*^{tm1Wjl} Tg(CMV-IL3,CSF2,KITLG)1Eav/MloySzJ, 013062) reconstituted with human CD34$^+$ hematopoietic stem cells were purchased from The Jackson Laboratory. The number of animals used in the experiments is presented in each figure. Mice received humane care in compliance with the *Guide for the Principles of Laboratory Animals*. Animal experiments were approved by the University of California, San Francisco (UCSF) Institutional Animal Care and Use Committee and performed according to local guidelines.

Methods for mouse cells

Mouse iPSC culture. All iPSCs were grown on mouse embryonic fibroblast (MEF) feeder cells in KO DMEM 10829 with 15% KO Serum Replacement, supplemented with 1% glutamine, 1% MEM-NEAA, 1% penicillin–streptomycin (all Gibco), 0.2% beta-mercaptoethanol and 100 U of leukemia inhibitory factor (LIF) (both Millipore). Medium was changed daily, and the cells were passaged every 2–3 days using 0.05% trypsin-EDTA (Gibco). Cell cultures were regularly screened for mycoplasma infections using the MycoAlert Kit (Lonza). B6 iPSCs were transduced to express Fluc. Then, 100,000 iPSCs were plated in one gelatin-coated six-well plate and incubated overnight at 37 °C in 5% CO_2. Medium was changed the next day, and one vial of Fluc lentiviral particles expressing luciferase II gene under the re-engineered EF1a promoter (Gentarget) was added. One milliliter of cell medium was added after 36 hours. Then, 24 hours later, complete media change was performed, and, after another 2 days, luciferase expression was confirmed by adding D-luciferin (Promega). Signals were quantified with Spectral Imaging AMI (Spectral Instruments) in maximum photons per second per centimeter square per steradian (p/s/cm^2/sr). B6 iPSC gene editing to engineer B6 HIP iPSCs was performed as described[6].

EC differentiation of iPSCs. To initiate the differentiation of mouse iPSCs to ECs, medium was changed to RPMI-1640 containing 2% B-27 minus insulin (both Gibco) and 5 µM CHIR-99021 (Selleckchem). Starting on day 2, RPMI-1640 containing 2% B-27 minus insulin (both Gibco) and 2 µM CHIR-99021 (Selleckchem) was used. From day 4 to day 7, cells were exposed to RPMI-1640 EC medium containing 2% B-27 minus insulin plus 50 ng ml^{-1} of mouse vascular endothelial growth factor (mVEGF, R&D Systems), 10 ng ml^{-1} of mouse fibroblast growth factor basic (mFGFb, R&D Systems), 10 µM Y-27632 (Sigma-Aldrich) and 1 µM SB 431542 (Sigma-Aldrich). EC clusters were visible from day 7, and cells were maintained in Endothelial Cell Basal Medium 2 (PromoCell) plus supplements, 10% FCS heat-inactivated (HI) (Gibco), 1% penicillin–streptomycin, 25 ng ml^{-1} of VEGF, 2 ng ml^{-1} of FGFb, 10 µM Y-27632 (Sigma-Aldrich) and 1 µM SB 431542 (Sigma-Aldrich). The differentiation process was completed after 21 days, and undifferentiated cells were detached during the differentiation process. For purification, cells went through MACS purification using anti-CD15 mAb-coated magnetic microbeads (Miltenyi) for negative selection.

Transduction and sorting of mouse iECs. In a pre-coated 12-well plate, mouse iECs were plated at a density of 5×10^4 in EC media and then incubated overnight at 37 °C in 5% CO_2. The next day, cells were incubated overnight at 37 °C in 5% CO_2 with lentiviral particles carrying a transgene for mouse Cd64 (NM_010186, Gentarget, custom product), human CD64 (NM_000566, Origene, RC207487L2V) or human CD52 (NM_001803, Gentarget, custom product) at a multiplicity of infection (MOI) of 4. Polybrene (8 µg ml^{-1}, Millipore) was added to the media, and the plate was centrifuged at 800*g* for 30 minutes before overnight incubation. Cell populations were sorted on a FACSAria (BD Biosciences) for high expression of Cd64, CD64 or CD52 using BV421-labeled anti-mouse Cd64 (FcγRI) antibody (clone X54-5/7.1, BioLegend, 139309, concentration 0.01 mg ml^{-1}), BV421-labeled anti-human CD64 antibody (clone 10.1, BD Biosciences, 562872, concentration 0.01 mg ml^{-1}) or APC-conjugated anti-human CD52 antibody (clone HI186, BioLegend, 316008, concentration 0.005 mg ml^{-1}), respectively.

Flow cytometry analysis. For the detection of MHC class I and II surface expression on iECs, cells were stimulated with 100 ng ml^{-1} of IFN-γ and 100 ng ml^{-1} of TNFα (both PeproTech) for 48 hours. Cells were harvested and labeled with flow cytometry antibodies for MHC class I (clone AF6-88.5.5.3, eBioscience, 46-5958-82, concentration 0.01 mg ml^{-1}) or mouse IgG2a isotype-matched control antibody (clone eBM2a, eBioscience, 46-4724-80, concentration 0.01 mg ml^{-1}), MHC class II (clone M5/114.15.2, eBioscience, 46-5321-82, concentration 0.01 mg ml^{-1}) or rat IgG2b isotype-matched control antibody (clone eB149/10H5, eBioscience, 46-4031-80, concentration 0.01 mg ml^{-1}), Cd47 (clone miap301, BD Biosciences, 563584, concentration 0.01 mg ml^{-1}) or rat IgG2a isotype-matched control antibody (clone R35-95, BD Biosciences, 557690, concentration 0.01 mg ml^{-1}). Surface expression of Cd64, CD64 or CD52 was assessed using the antibodies listed above.

To assess mouse Cd64-F$_c$ receptor binding, mouse iECs were incubated with different concentrations of mouse IgG2a anti-CD20 (clone rIGEL/773, Abcam, ab219329) and QDot655-labeled F(ab′)2-goat anti-mouse IgG secondary antibody (Thermo Fisher Scientific, Q-11021MP, concentration 0.002 mg ml^{-1}). Similarly, human CD64-F$_c$ receptor binding was assessed with a humanized IgG1 anti-CD52 (alemtuzumab, ichorbio, ICH4002) and QDot655-labeled F(ab′)2-goat anti-human IgG secondary antibody (Thermo Fisher Scientific, Q-11221MP, concentration 0.002 mg ml^{-1}). Cells were analyzed on a LSRFortessa (BD Biosciences), and results were expressed as fold change to isotype-matched control Ig staining. FlowJo 10 was used to analyze flow cytometric data.

Mouse NK cell isolation. C57BL/6 mice were stimulated with poly I:C injections (100 µg intraperitoneally, Sigma-Aldrich) and, 18 hours later, NK cells were isolated from spleens. After red blood cell lysis, NK cells were purified using the MagniSort Mouse NK Cell Enrichment Kit (Invitrogen), followed by CD49b MACS-sorting (Miltenyi). This mouse NK cell population had a purity of >99%.

XCelligence killing assays. Real-time killing assays were performed on the XCelligence SP platform and MP platform (ACEA Biosciences). Special 96-well E-plates (ACEA Biosciences) coated with collagen (Sigma-Aldrich) were used. A total of 4×10^4 mouse iECs were plated in 100 µl of medium. After the cell index reached 0.7, we added 4×10^4 C57BL/6 6 NK cells to ADCC assays or 50 µl of C57BL/6 serum to CDC assays. The following antibodies were used and added after mixing with the NK cells in 50 µl of medium or in the serum as indicated: mouse IgG2a anti-H-2^b (BioXCell, clone AF6-88.5.5.3, BE0121) and humanized anti-CD52 IgG1 (alemtuzumab, ichorbio, ICH4002). Different concentrations ranging from 0.0001 µg ml^{-1} to 1 µg ml^{-1} were used. As a negative control, cells were treated with 2% Triton X-100 in medium. Data were standardized and analyzed with RTCA Pro 2.3.2 software (ACEA Biosciences).

Survival analysis of mouse iECs using BLI. One million firefly Luc$^+$ B6 HIP iECs^{CD52} and B6 HIP iECs^{CD52,CD64} were transplanted subcutaneously, and 1 mg of alemtuzumab was injected into the peritoneum on post-transplant days 0 and 3. For imaging, D-luciferin firefly potassium salt (375 mg kg^{-1}, Biosynth) was dissolved in PBS (pH 7.4, Gibco), and 250 µl was injected intraperitoneally in anesthetized mice. Animals were imaged in the AMI HT (Spectral Instruments). Region of interest (ROI) bioluminescence was quantified in units of maximum p/s/cm^2/sr. The maximum signal from an ROI was measured using Aura Imaging software (Spectral Instruments).

Methods for human cells

Human iPSC culture. Human iPSCs were cultured on diluted feeder-free Matrigel-coated 10-cm dishes (hESC qualified, BD Biosciences) in Essential 8 Flex Medium (Thermo Fisher Scientific). Medium was changed every 24 hours, and Versene (Gibco) was used for cell passaging at a ratio of 1:6. For luciferase transduction, 1×10^5 iPSCs were plated in one six-well plate and grown overnight at 37 °C in 5% CO_2. Medium was changed the next day, and 200 µl of Fluc lentiviral particles expressing luciferase II gene under re-engineered EF1a promotor (Gentarget) was added. After 36 hours, 1 ml of cell medium was added. After another 24 hours, complete medium change was performed. Then, 2 days later, luciferase expression was confirmed by adding D-luciferin (Promega). Signals were quantified in p/s/cm^2/sr. Human iPSC gene editing to engineer HIP iPSCs was performed as described[6].

Endothelial cell differentiation from human iPSCs. When the iPSC confluency reached 60%, the differentiation was initiated, and medium was changed to RPMI-1640 containing 2% B-27 minus insulin (both Gibco) and 5 µM CHIR-99021 (Selleckchem). On day 2, the medium was changed to RPMI-1640 containing 2% B-27 minus insulin (Gibco) and 2 µM CHIR-99021 (Selleckchem). From culture day 4 to day 7, cells were exposed to RPMI-1640 EC medium, RPMI-1640 containing 2% B-27 minus insulin plus 50 ng ml^{-1} of VEGF (PeproTech), 10 ng ml^{-1} of human FGFb (PeproTech), 10 µM Y-27632 (Sigma-Aldrich) and 1 µM SB 431542 (Sigma-Aldrich). EC clusters were visible from day 7, and cells were maintained in Endothelial Cell Basal Medium 2 (PromoCell) plus supplements, 10% FCS HI (Gibco), 1% penicillin–streptomycin, 25 ng ml^{-1} of VEGF, 2 ng ml^{-1} of FGFb, 10 µM Y-27632 (Sigma-Aldrich) and 1 µM SB 431542 (Sigma-Aldrich). The differentiation protocol was completed after 14 days, and undifferentiated cells were detached during the differentiation process. TrypLE (Gibco) was used for passaging the cells 1:3 every 3–4 days.

NK cell culture. Human primary NK cells were purchased from STEMCELL Technologies (70036) and cultured in RPMI-1640 plus 10% FCS HI and 1% penicillin–streptomycin before performing the assays.

Macrophage differentiation from PBMCs. PBMCs were isolated by Ficoll separation from fresh blood and re-suspended in RPMI-1640 with 10% FCS HI and 1% penicillin–streptomycin (all Gibco). Cells were plated in 24-well plates at a concentration of 1×10^6 cells per milliliter, and 10 ng ml^{-1} of human M-CSF (PeproTech) was added to the medium. Medium was changed every other day. From day 6 onward, 1 µg ml^{-1} of human IL-2 (PeproTech) was added to the medium for 24 hours before performing assays.

Human thyroid epithelial cells. Immortalized human thyroid epiCs were purchased from InSCREENex (INS-CI-1017) and cultured in the media provided from the manufacturer (INS-ME-1017, InSCREENex). The cells were maintained in culture and passaged using TryplE 1:3 every 3–4 days.

Human pancreatic beta cells. Human iPSC-derived pancreatic beta cells were purchased from Takara Bio (ChiPSC22, Y10106) and cultured in Cellartis hiPS Beta Cell Media Kit (Takara Bio, Y10108). Cells were plated in 12-well plates according to the manufacturer's protocol. Some cells were transduced with CD64t lentiviral particles (Gentarget).

Human CAR T cells. Human anti-CD19 CAR T cells were generated from human PBMCs using lentiviral particles carrying a transgene for the CD19 scFv-4-1BB-CD3ζ construct (ProMab, PM-CAR1002-V). PBMCs were stimulated with IL-2 overnight and seeded in 96-well U-bottom plates at a density of 10^5 cells per well containing protamine sulfate and 0.1 µg ml^{-1} of IL-2 (PeproTech). Lentiviruses were added to the wells at an MOI of 20. Some wells were transduced additionally with CD64t lentiviral particles at an MOI of 20 (Gentarget). Spinfection was carried out at 1,800 r.p.m. for 30 minutes at 25 °C. After that, the cells were returned to a humidified 5% CO_2 incubator overnight. Medium was changed after 2 days, and cells were seeded at a density of 10^6 per milliliter in T cell media (OpTmizer, Thermo Fisher Scientific). CD3/CD28 beads (Thermo Fisher Scientific) were used for T cell expansion. Cells were sorted for CAR$^+$ and CAR$^+$/CD64t$^+$ populations on a BD FACSAria Fusion and used for further assays.

Transduction and sorting of human cells. In a pre-coated 12-well plate, human iECs, thyroid epiCs or beta cells were plated at a density of 5×10^4 in cell-specific media and then incubated overnight at 37 °C in 5% CO_2. The next day, cells were incubated overnight at 37 °C in 5% CO_2 with lentiviral particles carrying a transgene for human CD52 (NM_001803, Gentarget, custom product), human CD64 (NM_000566, Origene, RC207487L2V), human TPO (NM_000547, Gentarget, custom product) or a truncated form of human CD64 (CD64t, ATGTGGTTCTTGACAACTCTGCTCCTTTGGGTTCCAGTTGATGGGCAAGTGGACACCACAAAGGCAGTGATCACTTTGCAGCCTCCATGGGTCAGCGTGTTCCAAGAGGAAACCGTAACCTTGCACTGTGAGGTGCTCCATCTGCCTGGGAGCAGCTCTACACAGTGGTTTCTCAATGGCACAGCCACTCAGACCTCGACCCCCAGCTACAGAATCACCTCTGCCAGTGTCAATGACAGTGGTGAATACAGGTGCCAGAGAGGTCTCTCAGGGCGAAGTGACCCCATACAGCTGGAAATCCACAGAGGCTGGCTACTACTGCAGGTCTCCAGCAGAGTCTTCACGGAAGGAGAACCTCTGGCCTTGAGGTGTCATGCGTGGAAGGATAAGCTGGTGTACAATGTGCTTTACTATCGAAATGGCAAAGCCTTTAAGTTTTTCCACTGGAATTCTAACCTCACCATTCTGAAAACCAACATAAGTCACAATGGCACCTACCATTGCTCAGGCATGGGAAAGCATCGCTACACATCAGCAGGAATATCTGTCACTGTGAAAGAGCTATTTCCAGCTCCAGTGCTGAATGCATCTGTGACATCCCCACTCCTGGAGGGGAATCTGGTCACCCTGAGCTGTGAAACAAAGTTGCTCTTGCAGAGGCCTGGTTTGCAGCTTTACTTCTCCTTCTACATGGGCAGCAAGACCCTGCGAGGCAGGAACACATCCTCTGAATACCAAATACTAACTGCTAGAAGAGAAGACTCTGGGTTATACTGGTGCGAGGCTGCCACAGAGGATGGAAATGTCCTTAAGCGCAGCCCTGAGTTGGAGCTTCAAGTGCTTGGCCTCCAGTTACCAACTCCTGTCTGGTTTCATGTCCTTTTCTATCTGGCAGTGGGAATAATGTTTTTAGTGAACACTGTTCTCTGGGTGACAATATAG, Gentarget, custom product) at an MOI of 4. Polybrene (8 µg ml^{-1}, Millipore) was added to the media, and the plate was centrifuged at 800*g* for 30 minutes before overnight incubation. Cell populations were sorted on a FACSAria (BD Biosciences) using APC-conjugated anti-human CD52 antibody (clone HI186, BioLegend, 316008, concentration 0.005 mg ml^{-1}), BV421-labeled anti-human CD64 antibody (clone 10.1, BD Biosciences, 562872, concentration 0.01 mg ml^{-1}), PE-conjugated anti-human TPO antibody (clone MoAb47, Santa Cruz Biotechnology, sc-58432, concentration 0.01 mg ml^{-1}) or FITC-conjugated anti-FMC63 scFv (clone Y45, Acro Biosystems, FM3-FY45, dilution 1:50).

CD64 knockdown in macrophages. Human peripheral blood macrophages were purchased from STEMCELL Technologies (70042) and seeded in 12-well plates at a density of 1×10^5 cells per well in RPMI-1640 media (Gibco) supplemented with 10% FCS HI (Sigma Aldrich). The next day, lentiviral particles with shRNA for human CD64 (custom order, Gentarget) were added to the media at an MOI 20, and 1 µg ml^{-1} of protamine sulfate was added. After 72 hours, the macrophages were harvested and sorted for CD64 deficiency using a BV421 mouse anti-human CD64 antibody (clone 10.1, 562872, BD Biosciences, concentraztion 0.01 mg ml^{-1}) and the isotype-matched control mouse IgG1κ antibody (clone MOPC-21, 400157, BioLegend, concentration 0.01 mg ml^{-1}) on a FACSAria flow cytometer (BD Biosciences).

FcγRIIB expression in HIP iECs. A six-well plate was coated with gelatin, and 1×10^5 HIP iECs^{CD52} per well were seeded in 2.5 ml of EC media and incubated for 24 hours at 37 °C in 5% CO_2. The next day, 1 ml of fresh

EC media was added to the wells, and human FcγRIIB lentiviral particles (custom order, Gentarget) were added to the media at an MOI of 20, and 1 μg ml^{-1} of protamine sulfate was also added. After 24 hours, 1 ml of EC media was added to the cells, and, after subsequent 48 hours, a complete media change was performed. The cells were harvested and stained for FcγRIIB expression using an APC mouse anti-human CD32B/C antibody (clone S18005H, 398304, BioLegend, concentration 0.0025 mg ml^{-1}) together with the isotype-matched control APC mouse IgG1κ antibody (clone MOPC-21, 555751, BD Biosciences, concentration 0.0025 mg ml^{-1}). The FcγrIIB^{+} cells were sorted on a FACSAria flow cytometer (BD Biosciences).

Flow cytometry analysis. Human iPSCs were grown in six-well plates in medium containing 100 ng ml^{-1} of IFN-γ and 100 ng ml^{-1} of TNFα for 48 hours. Cells were harvested and labeled with APC-conjugated anti-HLA-A,B,C antibody (clone G46_2.6, BD Biosciences, 562006, concentration 0.05 mg ml^{-1}) for HLA class I detection or APC-conjugated IgG1 isotype-matched control antibody (clone MOPC-21, BD Biosciences, 555751, concentration 0.05 mg ml^{-1}). For HLA class II detection, cell were labeled with Alexa Fluor 647-labeled anti-HLA-DR,DP,DQ antibody (clone Tu39, BD Biosciences, 563591, concentration 0.01 mg ml^{-1}) or Alexa Fluor 647-labeled IgG2a isotype-matched control antibody (clone G155-178, BD Biosciences, 557715, concentration 0.01 mg ml^{-1}). PerCP-Cy5.5-conjugated anti-CD47 (clone B6H12, BD Biosciences, 561261, concentration 0.01 mg ml^{-1}) or PerCP-Cy5.5-conjugated IgG1 isotype-matched control antibody (clone MOPC-21, BD Biosciences, 552834, concentration 0.01 mg ml^{-1}) were used for detection of CD47. For MICA detection, a humanized anti-MICA IgG1 (Creative Biolabs, TAB-0799CL, concentration 0.01 mg ml^{-1}) with PE-labeled mouse anti-human IgG1 F_c secondary antibody (clone HP6001, SouthernBiotech, 9054-09, concentration 0.01 mg ml^{-1}) was used. For SIRPα detection, an APC-labeled mouse anti-human SIRPα (clone 15-414, 372106, BioLegend, concentration 0.02 mg ml^{-1}) with IgG2aκ isotype-matched control antibody (557715, BD Biosciences, concentration 0.02 mg ml^{-1}) was used. Surface expression of CD52, CD64/CD64t, TPO and anti-CD19 scFv was assessed using the antibodies listed above. To study competing CD52 binding, an APC-conjugated anti-CD52 mouse IgG2b was used (clone HI186, GTX80134, GeneTex).

To assess human CD64-F_c binding, a humanized IgG1 anti-CD52 (alemtuzumab, ichorbio, ICH4002), a humanized IgG1 anti-TPO (clone B8, Creative Biolabs, FAMAB-0014JF) or humanized anti-SIRPα antibodies (clone KWAR23, IgG1, IgG2, IgG3 or IgG4, custom order, Creative Biolabs) and QDot655-labeled F(ab′)2-goat anti-human IgG secondary antibody (Thermo Fisher Scientific, Q-11221MP, 0.002 mg ml^{-1}) were used.

To assess alemtuzumab internalization, cells were incubated with 1 μg ml^{-1} of Alexa Fluor 488-conjugated anti-CD52 (clone Hu116, FAB9889G, R&D Systems) for different time periods. Then, an anti-Alexa Fluor 488 quenching antibody (Invitrogen, A-11094) was used at 10 μg ml^{-1} for 30 minutes. Flow cytometry of cells with and without the quenching antibody was done to assess total and intracellular fluorescence, respectively. Cells were analyzed on a LSR-Fortessa (BD Biosciences), and results were expressed as fold change to isotype-matched control Ig staining.

XCelligence killing assays. Real-time killing assays were performed on the XCelligence SP platform and MP platform (ACEA Biosciences). Special 96-well E-plates (ACEA Biosciences) coated with gelatin (Sigma-Aldrich) were used. A total of 4×10^4 human iECs, epiCs, beta cells, CAR T cells or macrophages were plated in 100 μl of medium. After the cell index reached 0.7, we added 4×10^4 human NK cells to ADCC assays or 50 μl of blood-type-compatible human serum to CDC assays. Patient serum samples were treated with DTT to eliminate blood type IgM antibodies before use. For NALM killing assays, 4×10^4 NALM cells were plated, and 4×10^4 CAR T cells were used as effector cells. The following antibodies were used and added after mixing with the NK cells in 50 μl of medium or in the serum as indicated: humanized anti-CD52 IgG1 (alemtuzumab, ichorbio, ICH4002), humanized anti-MICA IgG1 (Creative Biolabs, TAB-0799CL), humanized anti-HLA-A2 IgG1 (clone 3PF12, Absolute Antibody, AB00947-10.0), humanized anti-Rh(D) IgG1 (clone F5, Creative Biolabs, FAMAB-0089WJ), humanized anti-TPO IgG1 (clone B8, Creative Biolabs, FAMAB-0014JF), humanized anti-CD3 IgG1 (Creative Biolabs, custom product) and humanized anti-CD19 scFv (FMC63) IgG1 (clone 136.20.1, Creative Biolabs, HPAB-0440-YJ-m/h). Different concentrations ranging from 0.0001 μg ml^{-1} to 1 μg ml^{-1} were used. As a negative control, cells were treated with 2% Triton X-100 in medium (data not shown). Data were standardized and analyzed with RTCA software (ACEA Biosciences).

Ex vivo T cell priming. Blood from an HLA-A2^{-} donor was collected, and PBMCs were obtained after Ficoll separation. The PBMCs were primed by co-culturing 5×10^5 HLA-A2^{+} wild-type iEC cells and 1×10^6 PBMCs in gelatin-coated flasks. The media, which consisted of a 1:1 mixture of EC medium and PBMC medium, was changed every 3 days. After 14 days, the cells in suspension were harvested and sorted using an APC mouse anti-human CD3 antibody (clone SP34-2, 557597, BD Biosciences, concentration 0.01 mg ml^{-1}) together with the isotype-matched control APC mouse IgG1κ antibody (clone MOPC-21, 550854, BD Biosciences, concentration 0.01 mg ml^{-1}) and a BV421 mouse anti-human CD8 antibody (clone SK1, 344748, BioLegend, concentration 0.005 mg ml^{-1}) together with the isotype-matched control mouse IgG1κ antibody (clone MOPC-21, 400157, BioLegend, concentration 0.005 mg ml^{-1}). The CD3^{+}CD8^{+} cells were sorted using a FACSAria flow cytometer (BD Biosciences) and used for real-time XCelligence killing assays with the anti-HLA-A2 IgG1 antibody, with or without prior treatment with anti-CD20 IgG1.

Survival analysis of human iECs using BLI. A total of 5×10^4 HIP iECs^{CD52} or HIP iECs^{CD52,CD64} were injected subcutaneously into NSG mice or humanized NSG-SGM3 mice mixed together with 1 million human NK cells with or without 1 mg of alemtuzumab. On the two subsequent days, 1-mg doses of alemtuzumab were injected subcutaneously into the vicinity of the cell transplants where indicated. Transplant experiments with human thyroid epiCs^{TPO} and epiCs^{TPO,CD64t} or human beta cells and beta cells^{CD64t} were similarly performed in NSG mice with anti-TPO IgG1 or anti-HLA-A2 IgG1, respectively. All injected cells were Luc^{+}. For imaging, D-luciferin firefly potassium salt (375 mg kg^{-1}, Biosynth) was dissolved in PBS (pH 7.4, Gibco), and 250 μl was injected intraperitoneally in anesthetized mice. Animals were imaged in the AMI HT (Spectral Instruments). ROI bioluminescence was quantified in units of maximum p/s/cm^2/sr. The maximum signal from an ROI was measured using Aura Imaging software (Spectral Instruments).

In vivo cytotoxicity assay with adoptive transfer. Five million DiO-labeled HIP iECs^{CD52} and 5 million DiD-labeled HIP iECs^{CD52,CD64} were mixed and injected intraperitoneally into NSG mice (Vybrant Multicolor Cell-Labeling Kit, Thermo Fisher Scientific). A total of 10^8 IL-2-stimulated human primary NK cells (STEMCELL Technologies) or 10^8 macrophages (differentiated from PBMCs) were also intraperitoneally injected. Human primary NK cells were pre-treated with human IL-2 (1 μg ml^{-1}, PeproTech) for 12 hours before injection. After 48 hours, cells were collected from the peritoneum, and the ratio of both cell populations was assessed by flow cytometry (FACSCalibur, BD Biosciences).

Thyroxine ELISA. A 96-well plate was coated with gelatin, and 3×10^4 human thyroid epiCs^{TPO} or epiCs^{TPO,CD64t} per well were seeded in 100 μl of h7H media[49] and incubated for 24 hours at 37 °C in 5% CO_2. The next day, the h7H media was changed and supplemented with 1 mU ml^{-1} of native bovine thyroid-stimulating hormone (TSH) protein (TSH-1315B, Creative BioMart). Three wells per epiC group were also supplemented with 1 μg ml^{-1} of anti-CD52 IgG1 (alemtuzumab, clone Campath-1H,

Bio-Rad). After 72 hours, the supernatant was collected, and the level of thyroxine was assessed using the thyroxine (T4) competitive ELISA kit (EIAT4C, Invitrogen) according to the manufacturer's instructions. Results are presented as change in optical density (OD) between groups with and without alemtuzumab.

Insulin ELISA. A 24-well plate was coated with gelatin, and 5×10^4 iPSC-derived beta cells and beta cells^{CD64t} (Y10108, Takara Bio) per well were seeded in 500 µl of Cellartis hiPS beta cell media and incubated for 24 hours at 37 °C in 5% CO_2. The next day, the Cellartis hiPS beta cell media was changed to RPMI-1640 without glucose (11879-020, Gibco) for 2 hours. After 2 hours, the media was changed to RPMI without glucose supplemented with 2 mM glucose (G7528, Sigma-Aldrich). Three wells per beta cell group were also supplemented with 1 µg ml^{-1} of anti-CD52 IgG1 (alemtuzumab, clone Campath-1H, MCA6101, Bio-Rad). After 20 minutes, the supernatant was collected, and the media was changed to RPMI without glucose supplemented with 20 mM glucose. Again, 1 µg ml^{-1} of alemtuzumab was added to three wells per group. After 20 minutes, the supernatant was collected, and the level of human insulin was determined using the human insulin ELISA kit (KAQ1251, Invitrogen) according to the manufacturer's instructions. Results are presented as change in OD between groups with and without alemtuzumab.

Statistics

All data are expressed as mean ± s.d. Intergroup differences were appropriately assessed by either unpaired Student's *t*-test or one-way ANOVA with Bonferroni's post hoc test. To determine if the effect of anti-CD52 concentration on fluorescence intensity differed significantly by antibody type, linear regression was performed with mean fluorescence intensity as the dependent variable and an interaction term for antibody type (anti-CD52 versus anti-CD20) by ten-fold increase units of anti-CD52 concentration (µg ml^{-1}). Hypothesis tests were two-sided, and the significance threshold was set to 0.05. To determine if the cell lines differed significantly in their capacity to internalize alemtuzumab, linear regression was performed with percentage of internalized alemtuzumab as the dependent variable and an interaction term for cell line (hiECs^{CD52} versus hiECs^{CD52,CD64}) by time after exposure to alemtuzumab. Exposure to alemtuzumab was treated as a continuous variable (1 = 10 minutes, 2 = 2 hours, 3 = 24 hours). Hypothesis tests were two-sided, and the significance threshold was set to 0.05. Statistical analyses were performed using SAS version 9.4.

Reporting summary

Further information on research design is available in the Nature Research Reporting Summary linked to this article.

Data availability

All data generated or analyzed during this study are included in this published article and its Supplementary Information files. No pre-established data exclusion method was used. No clinical data were included. Supplementary Information is available in the online version of the paper.

References

49. Bravo, S. B. et al. Humanized medium (h7H) allows long-term primary follicular thyroid cultures from human normal thyroid, benign neoplasm, and cancer. *J. Clin. Endocrinol. Metab.* **98**, 2431–2441 (2013).

Acknowledgements

Special thanks to B. Nelson (Spectral Instruments) for technical support. Medical illustration was done by J. A. Klein of Mito Pop. Statistical support was expertly provided by A. Shui and the Biostatistics Core, which is funded by the UCSF Department of Surgery.

Author contributions

A.G. performed lentiviral transductions and cell sorting, immune killing assays and imaging studies. G.T. performed cell injections and imaging studies. R.R. provided transplant serum samples and gave technical support and conceptual advice. Z.Q. provided endocrine patient serum samples and gave technical support and conceptual advice. C.D. gave technical support and conceptual advice. S.S. established immune assays. T.D. designed the experiments, supervised the project and wrote the manuscript.

Competing interests

Sana Biotechnology, Inc. has an exclusive license on the HIP cell technology. S.S. is currently an employee of Sana Biotechnology, Inc. S.S. and T.D. own stock in Sana Biotechnology, Inc. Neither a reagent nor any funding from Sana Biotechnology, Inc. was used in this study. The University of California, San Francisco has filed patent applications that cover these inventions. Correspondence and requests for materials should be addressed to T.D. (tobias.deuse@ucsf.edu).

Additional information

Supplementary information The online version contains supplementary material available at https://doi.org/10.1038/s41587-022-01540-7.

Correspondence and requests for materials should be addressed to Tobias Deuse.

Peer review information *Nature Biotechnology* thanks the anonymous reviewers for their contribution to the peer review of this work.

Reprints and permissions information is available at www.nature.com/reprints.

nature portfolio

Corresponding author(s): Tobias Deuse

Last updated by author(s): Sep 26, 2022

Reporting Summary

Nature Portfolio wishes to improve the reproducibility of the work that we publish. This form provides structure for consistency and transparency in reporting. For further information on Nature Portfolio policies, see our Editorial Policies and the Editorial Policy Checklist.

Statistics

For all statistical analyses, confirm that the following items are present in the figure legend, table legend, main text, or Methods section.

n/a	Confirmed
☐	☒ The exact sample size (*n*) for each experimental group/condition, given as a discrete number and unit of measurement
☐	☒ A statement on whether measurements were taken from distinct samples or whether the same sample was measured repeatedly
☐	☒ The statistical test(s) used AND whether they are one- or two-sided *Only common tests should be described solely by name; describe more complex techniques in the Methods section.*
☒	☐ A description of all covariates tested
☒	☐ A description of any assumptions or corrections, such as tests of normality and adjustment for multiple comparisons
☐	☒ A full description of the statistical parameters including central tendency (e.g. means) or other basic estimates (e.g. regression coefficient) AND variation (e.g. standard deviation) or associated estimates of uncertainty (e.g. confidence intervals)
☐	☒ For null hypothesis testing, the test statistic (e.g. *F*, *t*, *r*) with confidence intervals, effect sizes, degrees of freedom and *P* value noted *Give P values as exact values whenever suitable.*
☒	☐ For Bayesian analysis, information on the choice of priors and Markov chain Monte Carlo settings
☒	☐ For hierarchical and complex designs, identification of the appropriate level for tests and full reporting of outcomes
☒	☐ Estimates of effect sizes (e.g. Cohen's *d*, Pearson's *r*), indicating how they were calculated

Our web collection on statistics for biologists contains articles on many of the points above.

Software and code

Policy information about availability of computer code

Data collection	FlowJo 10 was used to analyze flow cytometric data. Prism9 was used for graphing and statistical analysis. Aura 3.2 was used for quantification of bioluminescence imaging. XCelligence assays were measured with the RTCA software.
Data analysis	Data were automatically analyzed in the mentioned software above for RTCA. Statistical analysis was performed on Prism9 or SAS version 9.4.

For manuscripts utilizing custom algorithms or software that are central to the research but not yet described in published literature, software must be made available to editors and reviewers. We strongly encourage code deposition in a community repository (e.g. GitHub). See the Nature Portfolio guidelines for submitting code & software for further information.

Data

Policy information about availability of data

All manuscripts must include a data availability statement. This statement should provide the following information, where applicable:

- Accession codes, unique identifiers, or web links for publicly available datasets
- A description of any restrictions on data availability
- For clinical datasets or third party data, please ensure that the statement adheres to our policy

All data generated or analyzed during this study are included in this published article (and its supplementary information files). No pre-established data exclusion method was used. No clinical data were included. Supplementary Information is available in the online version of the paper.

Field-specific reporting

Please select the one below that is the best fit for your research. If you are not sure, read the appropriate sections before making your selection.

☒ Life sciences ☐ Behavioural & social sciences ☐ Ecological, evolutionary & environmental sciences

For a reference copy of the document with all sections, see nature.com/documents/nr-reporting-summary-flat.pdf

Life sciences study design

All studies must disclose on these points even when the disclosure is negative.

Sample size	The sample size for the in vivo studies to achieve statistical significance was not calculated before the studies as the survival of the HIP cells with or without human CD64 or mouse Cd64 in the different models was unknown prior. It was reasoned that 5-6 mice per group in individual experiments would indicate valid efficacy. No statistical test was used for the in vivo studies. Sample sizes in vitro were determined by three or more samples for comparisons between one or multiple groups, followed by the statistical test, where indicated. Again, the sample size to achieve statistical significance was not calculated before the studies for the reason described above.
Data exclusions	No pre-established data exclusion method was used.
Replication	The experimental findings can be reliably reproduced. Some key data generated by one co-author were repeated by other co-authors. The figure legends specify how often the experiments had been repeated.
Randomization	Some samples were number coded until the readout was finalized. The numbers were assigned prior to the experiment and determined the group/ treatment/ condition. Mice were number coded and randomly assigned to a group prior to the surgical procedure.
Blinding	For in vivo imaging, investigators doing the readouts were blinded and referred to the mice by their assigned numbers, which could later reveal the group they were in. For in vitro studies, usually different investigators performed the assay or did the analyses. The statistician is part of the UCSF core facility, not part of our lab, and unfamiliar with the science.

Reporting for specific materials, systems and methods

We require information from authors about some types of materials, experimental systems and methods used in many studies. Here, indicate whether each material, system or method listed is relevant to your study. If you are not sure if a list item applies to your research, read the appropriate section before selecting a response.

Materials & experimental systems

n/a	Involved in the study
☐	☒ Antibodies
☐	☒ Eukaryotic cell lines
☒	☐ Palaeontology and archaeology
☐	☒ Animals and other organisms
☒	☐ Human research participants
☒	☐ Clinical data
☒	☐ Dual use research of concern

Methods

n/a	Involved in the study
☒	☐ ChIP-seq
☐	☒ Flow cytometry
☒	☐ MRI-based neuroimaging

Antibodies

Antibodies used

Flow cytometry antibodies for mouse cells: BV421-labeled anti-mouse Cd64 (FcγRI) antibody (clone X54-5/7.1, Biolegend, catalog no. 139309), BV421-labeled anti-human CD64 antibody (clone 10.1, BD Biosciences, catalog no. 305002), APC-conjugated anti-human CD52 antibody (clone HI186, Biolegend, catalog no. 316008), anti-MHC class I (clone AF6-88.5.5.3, eBioscience, catalog no. 46-5958-82) or mouse IgG2a isotype-matched control antibody (clone eBM2a, eBioscience, catalog no. 46-4724-80), anti-MHC class II (clone M5/114.15.2, eBioscience, catalog no. 46-5321-82) or mouse IgG2b isotype-matched control antibody (clone eB149/10H5, eBioscience, catalog no. 46-4031-80), anti-mouse-Cd47 (clone miap301, BD Biosciences, catalog no. 563584) or rat IgG2a isotype-matched control antibody (clone R35-95, BD Biosciences, catalog no. 557690).

Flow cytometry antibodies for human cells: APC-conjugated anti-human CD52 antibody (clone HI186, Biolegend, catalog no. 316008), BV421-labeled anti-human CD64 antibody (clone 10.1, BD Biosciences, catalog no. 562872), PE-conjugated anti-human TPO antibody (clone MoAb47, Santa Cruz Biotechnology, catalog no. sc-58432), FITC-conjugated anti-FMC63 scFv (clone Y45, Acro Biosystems, catalog no. FM3-FY45), APC-conjugated anti-HLA-A,B,C antibody (clone G46_2.6,BD Biosciences, catalog no. 562006) or APC-conjugated IgG1 isotype-matched control antibody (clone MOPC-21, BD Biosciences, catalog no. 555751), Alexa-flour647-labeled anti-HLA-DR,DP,DQ antibody (clone Tu39, BD Biosciences, catalog no. 563591) or Alexa-flour647-labeled IgG2a isotype-matched control antibody (clone G155-178, BD Biosciences, catalog no. 557715), PerCP-Cy5.5-conjugated anti-CD47 (clone B6H12, BD Biosciences, catalog no. 561261) or PerCP-Cy5.5-conjugated IgG1 isotype-matched control antibody (clone MOPC-21, BD Biosciences, catalog no. 552834), humanized anti-MICA IgG1 (Creative Biolabs, catalog no. TAB-0799CL) with PE-labeled mouse anti-human IgG1

Fc secondary antibody (clone HP6001, Southern Biotech, catalog no. 9054-09), APC-conjugated anti-human CD32B/C antibody (clone S18005H, Biolegend, catalog no. 398303) AlexaFluor488-conjucated anti-CD52 (clone Hu116, catalog no. FAB9889G, R&D Systems), anti-AlexaFluor488 quenching antibody (Invitrogen, catalog no. A-11094). To study competing CD52 binding, an APC-conjugated anti-CD52 mouse IgG2b was used (clone HI186, catalog no. GTX80134, GeneTex, Irvine, CA).

Antibodies to assess mouse Cd64-Fc binding: mouse IgG2a anti-CD20 (clone rIGEL/773, Abcam, ab219329) and QDot655-labeled F(ab')2-goat anti-mouse IgG secondary antibody (ThermoFisher, catalog no. Q-11021MP). Antibodies to assess human CD64-Fc binding: humanized IgG1 anti-CD52 (alemtuzumab, ichorbio, catalog no. ICH4002) and QDot655-labeled F(ab')2-goat anti-human IgG secondary antibody (Thermo Fisher Scientific, catalog no. Q-11221MP).

Antibodies to assess human CD64-Fc binding: humanized IgG1 anti-CD52 (alemtuzumab, ichorbio, catalog no. ICH4002), humanized IgG1 anti-TPO (clone B8, Creative Biolabs, catalog no. FAMAB-0014JF) and QDot655-labeled F(ab')2-goat anti-human IgG secondary antibody (Thermo Fisher Scientific, catalog no. Q-11221MP), anti-SIRPalpha (clone KWAR23) human IgG1, IgG2, IgG3, and IgG4 (Creative Biolabs, custom order).

NK cell MACS sorting: The MagniSort Mouse NK cell Enrichment Kit (Invitrogen) was used followed by CD49b MACS-sorting (Miltenyi).

Antibodies for mouse in vitro killing assays: mouse IgG2a anti-H-2b (BioXCell, clone AF6-88.5.5.3, catalog no. BE0121), humanized anti-CD52 IgG1 (alemtuzumab, ichorbio, catalog no. ICH4002).

Antibodies for human in vitro killing assays: humanized anti-CD52 IgG1 (alemtuzumab, ichorbio, catalog no. ICH4002), humanized anti-MICA IgG1 (Creative Biolabs, catalog no. TAB-0799CL), humanized anti-HLA-A2 IgG1 (clone 3PF12, Absolute Antibody, catalog no. AB00947-10.0), humanized anti-Rh(D) IgG1 (clone F5, Creative Biolabs, catalog no. FAMAB-0089WJ), humanized anti-TPO IgG1 (clone B8, Creative Biolabs, catalog no. FAMAB-0014JF), humanized anti-CD3 IgG1 (Creative Biolabs, custom product), humanized anti-CD19 scFv (FMC63) IgG1 (clone 136.20.1, Creative Biolabs, catalog no. HPAB-0440-YJ-m/h), mouse anti-human CD52 IgG2b (MyBioSource, catalog no. MBS4158863).

Antibodies for in vivo killing assays: humanized anti-CD52 IgG1 (alemtuzumab, ichorbio, catalog no. ICH4002), humanized anti-HLA-A2 IgG1 (clone 3PF12, Absolute Antibody, catalog no. AB00947-10.0), humanized anti-TPO IgG1 (clone B8, Creative Biolabs, catalog no. FAMAB-0014JF).

Validation

Each antibody was tested with positive and negative control prior to staining the samples. Isotype and tested antibody were concentration matched. Antibody concentration were gathered from vendors datasheets:
MACS sorting
Anti-CD15 MACS-sorting (Miltenyi, https://www.miltenyibiotec.com/US-en/products/cd15-microbeads-human.html#gref), CD49b MACS-sorting (Miltenyi, https://www.miltenyibiotec.com/US-en/products/cd49b-antibody-anti-mouse-reafinity-rea541.html#apc:30-ug-in-200-ul).

Antibodies
BV421-labeled anti-mouse Cd64 ($Fc\gamma RI$) antibody (clone X54-5/7.1, Biolegend, catalog no. 139309, https://www.biolegend.com/en-us/products/brilliant-violet-421-anti-mouse-cd64-fcgammari-antibody-8992), BV421-labeled anti-human CD64 antibody (clone 10.1, BD Biosciences, catalog no. 562872, https://www.bdbiosciences.com/en-ca/products/reagents/flow-cytometry-reagents/research-reagents/single-color-antibodies-ruo/bv421-mouse-anti-human-cd64.562872), APC-conjugated anti-human CD52 antibody (clone HI186, Biolegend, catalog no. 316008, https://www.biolegend.com/en-us/products/apc-anti-human-cd52-antibody-3947), anti-MHC class I (clone AF6-88.5.5.3, eBioscience, catalog no. 46-5958-82, https://www.thermofisher.com/antibody/product/MHC-Class-I-H-2Kb-Antibody-clone-AF6-88-5-5-3-Monoclonal/46-5958-82), mouse IgG2a isotype-matched control antibody (clone eBM2a, eBioscience, catalog no. 46-4724-80, https://www.thermofisher.com/antibody/product/Mouse-IgG2a-kappa-clone-eBM2a-Isotype-Control/46-4724-80), anti-MHC class II (clone M5/114.15.2, eBioscience, Santa Clara, CA, catalog no. 46-5321-82, https://www.thermofisher.com/antibody/product/MHC-Class-II-I-A-I-E-Antibody-clone-M5-114-15-2-Monoclonal/46-5321-82), rat IgG2b isotype-matched control antibody (clone eB149/10H5, eBioscience, catalog no. 46-4031-80, https://www.thermofisher.com/antibody/product/Rat-IgG2b-kappa-clone-eB149-10H5-Isotype-Control/46-4031-80), anti-Cd47 (clone miap301, BD Biosciences, catalog no. 563584, https://www.bdbiosciences.com/en-ca/products/reagents/flow-cytometry-reagents/research-reagents/single-color-antibodies-ruo/alexa-fluor-647-rat-anti-mouse-cd47.563584), rat IgG2a isotype-matched control antibody (clone R35-95, BD Biosciences, catalog no. 557690, https://www.bdbiosciences.com/en-ca/products/reagents/flow-cytometry-reagents/research-reagents/flow-cytometry-controls-and-lysates/alexa-fluor-647-rat-igg2a-isotype-control.557690), APC-conjugated anti-human CD52 antibody (clone HI186, Biolegend, catalog no. 316008, https://www.biolegend.com/en-us/products/apc-anti-human-cd52-antibody-3947), BV421-labeled anti-human CD64 antibody (clone 10.1, BD Biosciences, catalog no. 562872, https://www.bdbiosciences.com/en-ca/products/reagents/flow-cytometry-reagents/research-reagents/single-color-antibodies-ruo/bv421-mouse-anti-human-cd64.562872), PE-conjugated anti-human TPO antibody (clone MoAb47, Santa Cruz Biotechnology, catalog no. sc-58432, https://www.scbt.com/p/thyroperoxidase-antibody-moab47), or FITC-conjugated anti-FMC63 scFv (clone Y45, Acro Biosystems, catalog no. FM3-FY45, https://www.acrobiosystems.com/P3228-FITC-Labeled-Monoclonal-Anti-FMC63-scFv-Antibody-Mouse-IgG1-%28Y45%29-DMF-Filed.html), BV421 mouse anti-human CD64 antibody (clone 10.1, catalog no. 562872, BD Biosciences, https://www.bdbiosciences.com/en-ca/products/reagents/flow-cytometry-reagents/research-reagents/single-color-antibodies-ruo/bv421-mouse-anti-human-cd64.562872), isotype-matched control mouse IgG1κ antibody (clone MOPC-21, catalog no. 400157, Biolegend, https://www.biolegend.com/en-us/products/brilliant-violet-421-mouse-igg1-kappa-isotype-ctrl-7194), APC mouse anti-human CD32B/C antibody (clone S18005H, catalog no. 398304, Biolegend, https://www.biolegend.com/en-us/products/apc-anti-human-cd32bc-antibody-19460), isotype-matched control APC mouse IgG1κ antibody (clone MOPC-21, catalog no. 555751, BD Biosciences, https://www.bdbiosciences.com/en-ca/products/reagents/flow-cytometry-reagents/research-reagents/flow-cytometry-controls-and-lysates/apc-mouse-igg1-isotype-control.555751), APC-conjugated anti-HLA-A,B,C antibody (clone G46_2.6,BD Biosciences, catalog no. 562006, https://www.bdbiosciences.com/en-ca/products/reagents/flow-cytometry-reagents/research-reagents/single-color-antibodies-ruo/apc-mouse-anti-human-hla-abc.562006), APC-conjugated IgG1 isotype-matched control antibody (clone MOPC-21, BD Biosciences, catalog no. 555751, https://www.bdbiosciences.com/en-ca/products/reagents/flow-cytometry-reagents/research-reagents/flow-cytometry-controls-and-lysates/apc-mouse-igg1-isotype-control.555751). Alexa-flour647-labeled anti-HLA-DR,DP,DQ antibody (clone Tu39, BD Biosciences, catalog no. 563591, https://www.bdbiosciences.com/en-ca/products/reagents/flow-cytometry-reagents/research-reagents/single-color-antibodies-ruo/alexa-fluor-647-mouse-anti-human-hla-dr-dp-dq.563591), Alexa-flour647-labeled IgG2a isotype-matched control antibody (clone G155-178, BD Biosciences, catalog no.

557715, https://www.bdbiosciences.com/en-ca/products/reagents/flow-cytometry-reagents/research-reagents/flow-cytometry-controls-and-lysates/alexa-fluor-647-mouse-igg2a-isotype-control.557715), PerCP-Cy5.5-conjugated anti-CD47 (clone B6H12, BD Biosciences, catalog no. 561261, https://www.bdbiosciences.com/en-ca/products/reagents/flow-cytometry-reagents/research-reagents/single-color-antibodies-ruo/percp-cy-5-5-mouse-anti-human-cd47.561261), PerCP-Cy5.5-conjugated IgG1 isotype-matched control antibody (clone MOPC-21, BD Biosciences, catalog no. 552834, https://www.bdbiosciences.com/en-ca/products/reagents/flow-cytometry-reagents/research-reagents/flow-cytometry-controls-and-lysates/percp-cy-5-5-mouse-igg1-isotype-control.552834), anti-MICA IgG1 (Creative Biolabs, catalog no. TAB-0799CL, https://www.creativebiolabs.net/Anti-MICA-Recombinant-Antibody-TAB-0799CL-27487.htm), PE-labeled mouse anti-human IgG1 Fc secondary antibody (clone HP6001, Southern Biotech, catalog no. 9054-09, https://www.southernbiotech.com/mouse-anti-human-igg1-fc-pe-hp6001-9054-09), APC-labeled mouse anti-human SIRP□ (clone 15-414, catalog no. 372106, Biolegend, https://www.biolegend.com/en-us/products/apc-anti-human-cd172a-sirpalpha-antibody-14165), IgG2a, □ isotype-matched control antibody (catalog no. 557715, BD Biosciences, https://www.bdbiosciences.com/en-ca/products/reagents/flow-cytometry-reagents/research-reagents/flow-cytometry-controls-and-lysates/alexa-fluor-647-mouse-igg2a-isotype-control.557715), APC mouse anti-human CD3 antibody (clone SP34-2, catalog no. 557597, BD Biosciences, https://www.bdbiosciences.com/en-ca/products/reagents/flow-cytometry-reagents/research-reagents/single-color-antibodies-ruo/apc-mouse-anti-human-cd3.557597), isotype-matched control APC mouse IgG1□ antibody (clone MOPC-21, catalog no. 550854, BD Biosciences, https://www.bdbiosciences.com/en-ca/products/reagents/flow-cytometry-reagents/research-reagents/flow-cytometry-controls-and-lysates/apc-mouse-igg1-isotype-control.550854), BV421 mouse anti-human CD8 antibody (clone SK1, catalog no. 344748, Biolegend, https://www.biolegend.com/en-us/products/brilliant-violet-421-anti-human-cd8-antibody-13512), isotype-matched control mouse IgG1□ antibody (clone MOPC-21, catalog no. 400157, Biolegend, https://www.biolegend.com/en-us/products/brilliant-violet-421-mouse-igg1-kappa-isotype-ctrl-7194), QDot655-labeled F(ab')2-goat anti-mouse IgG secondary antibody (ThermoFisher, catalog no. Q-11021MP, https://www.thermofisher.com/antibody/product/Goat-anti-Mouse-IgG-H-L-Secondary-Antibody-Polyclonal/Q-11021MP), QDot655-labeled F(ab')2-goat anti-human IgG secondary antibody (Thermo Fisher Scientific, catalog no. Q-11221MP, https://www.thermofisher.com/antibody/product/Goat-anti-Human-IgG-H-L-Secondary-Antibody-Polyclonal/Q-11221MP), QDot655-labeled F(ab')2-goat anti-human IgG secondary antibody (Thermo Fisher Scientific, catalog no. Q-11221MP, https://www.thermofisher.com/antibody/product/Goat-anti-Human-IgG-H-L-Secondary-Antibody-Polyclonal/Q-11221MP), mouse IgG2a anti-CD20 (clone rIGEL/773, Abcam, ab219329, https://www.abcam.com/cd20-antibody-rigel773-ab219329.html), humanized IgG1 anti-CD52 (alemtuzumab, ichorbio, catalog no. ICH4002, https://ichor.bio/product/alemtuzumab-biosimilar-research-grade-ich4002/), mouse IgG2a anti-H-2b (BioXCell, clone AF6-88.5.5.3, catalog no. BE0121, https://bxcell.com/product/h-2-k-b-2/), anti-FMC63 scFv (clone Y45, Acro Biosystems, catalog no. FM3-FY45, https://www.acrobiosystems.com/P3228-FITC-Labeled-Monoclonal-Anti-FMC63-scFv-Antibody-Mouse-IgG1-%28Y45%29-DMF-Filed.html), APC-conjugated anti-CD52 mouse IgG2b was used (clone HI186, catalog no. GTX80134, GeneTex, Irvine, CA, https://www.genetex.com/Product/Detail/CD52-antibody-HI186-APC/GTX80134), humanized IgG1 anti-TPO (clone B8, Creative Biolabs, catalog no. FAMAB-0014JF, https://www.creativebiolabs.net/anti-tpo-fab-fragment-clone-b8-137834.htm), AlexaFluor488-conjugated anti-CD52 (clone Hu116, catalog no. FAB9889G R&D Systems, https://www.rndsystems.com/products/human-cd52-research-grade-alemtuzumab-biosimilar-alexa-fluor-488-conjugated-antibody-hu116_fab9889g), anti-AlexaFluor488 quenching antibody (Invitrogen, catalog no. A-11094, https://www.thermofisher.com/antibody/product/Alexa-Fluor-488-Antibody-Polyclonal/A-11094), humanized anti-MICA IgG1 (Creative Biolabs, catalog no. TAB-0799CL, https://www.creativebiolabs.net/Anti-MICA-Recombinant-Antibody-TAB-0799CL-27487.htm), humanized anti-HLA-A2 IgG1 (clone 3PF12, Absolute Antibody, catalog no. AB00947-10.0, https://absoluteantibody.com/product/anti-hla-a2a28-3pf12/), humanized anti-Rh(D) IgG1 (clone F5, Creative Biolabs, catalog no. FAMAB-0089WJ, https://www.creativebiolabs.net/anti-rh-d-fab-fragment-clone-f5-131552.htm), humanized anti-TPO IgG1 (clone B8, Creative Biolabs, catalog no. FAMAB-0014JF, https://www.creativebiolabs.net/anti-tpo-fab-fragment-clone-b8-137834.htm), humanized anti-CD3 IgG1 (Creative Biolabs, custom product), humanized anti-CD19 scFv (FMC63) IgG1 (clone 136.20.1, Creative Biolabs, catalog no. HPAB-0440-YJ-m/h, https://www.creativebiolabs.net/anti-cd19-scfv-fmc63-recombinant-antibody-hpab-0440-yj-122546.htm).

Eukaryotic cell lines

Policy information about cell lines

Cell line source(s)	The Human Episomal iPSC Line was purchased from Thermo Fisher Scientific (Waltham, MA). Mouse iPSCs were reprogramed from C57BL/6 mice. Irradiated CF1 Mouse Embryonic Fibroblasts (MEFs) were used as feeder cells for mouse iPSCs and purchased from Thermo Fisher Scientific. Immortalized human thyroid epithelial cells (epiCs) were purchased from InScreenEx (catalog no. INS-CI-1017, Germany). Human iPSC-derived pancreatic beta cells were purchased from TaKaRa (ChiPSC22, catalog no. Y10106).
Authentication	None of the cell lines used have been authenticated.
Mycoplasma contamination	All cell lines were tested and negative for mycoplasma contamination using the Universal Mycoplasma test kit from ATCC.
Commonly misidentified lines (See ICLAC register)	No commonly misidentified cell lines were used.

Animals and other organisms

Policy information about studies involving animals; ARRIVE guidelines recommended for reporting animal research

Laboratory animals	C57BL/6 (C57BL/6J, B6, H2b, 000664, male, 6-12 weeks old), Rag-1 KO (B6.129S7-Rag1tm1Mom/J, 002216, male, 6-12 weeks old), and NSG (NOD.Cg-Prkdcscid Il2rgtm1Wjl/SzJ, 005557, female, 12-20 weeks old) and humanized NSG-SGM3 mice (NOD.Cg-Prkdcscid Il2rgtm1Wjl Tg(CMV-IL3,CSF2,KITLG)1Eav/MloySzJ, 013062, female, 12-20 weeks old) were purchased from the Jackson Laboratories

	(Sacramento, CA). Mice were housed in 12 hour light-dark cycles with humidity between 30-70% at ambient temperature of 68-79 degrees Fahrenheit.
Wild animals	No wild animals were used
Field-collected samples	No field collected samples were used
Ethics oversight	Mice received humane care in compliance with the Guide for the Principles of Laboratory Animals. Animal experiments were approved by the University of California San Francisco (UCSF) Institutional Animal Care and Use Committee and performed according to local guidelines.

Note that full information on the approval of the study protocol must also be provided in the manuscript.

Flow Cytometry

Plots

Confirm that:

☒ The axis labels state the marker and fluorochrome used (e.g. CD4-FITC).

☒ The axis scales are clearly visible. Include numbers along axes only for bottom left plot of group (a 'group' is an analysis of identical markers).

☒ All plots are contour plots with outliers or pseudocolor plots.

☒ A numerical value for number of cells or percentage (with statistics) is provided.

Methodology

Sample preparation	Cells were counted, stained and measured as single cell suspension in PBS+2% FCS hi.
Instrument	Cells were analyzed on the LSRFortessa (BD Bioscience) and results were expressed as fold-change to isotype-matched control Ig staining.
Software	The FlowJo software was used.
Cell population abundance	For flow cytometry analysis, more than 10,000 positive cells were measured. Cell sorting was gated for the desired population and sorted for the cell amount needed for assays.
Gating strategy	Samples were gated in FSC/SSC for the correct cell size and live cells. Isotype was measured for each sample as defined as unspecific staining threshold.

☐ Tick this box to confirm that a figure exemplifying the gating strategy is provided in the Supplementary Information.